第 40 卷 第 5 期
2025 年 10 月

新型炭材料（中英文）
New Carbon Materials

Cite this: New Carbon Materials, 2025, 40(5): 993-1015

Read Online

Review

Methods for the formation of M-N_x-C active sites on single-atom catalysts and their role in persulfate activation by non-radical paths

SI Wen-hao[1,2], SI Jin-xuan[3], WANG Kang-jun[2], QI Fei[1,*], CHEN Jia-bin[4,*], ZENG Ze-quan[1,*], HUANG Zhang-gen[1,5,*]

(1. *State Key Laboratory of Coal Conversion*, *Institute of Coal Chemistry*, *Chinese Academy of Sciences Taiyuan* 030001, *China*;
2. *College of Chemical Engineering*, *Shenyang University of Chemical Technology*, *Shenyang* 110142, *China*;
3. *School of Chemical Engineering and Technology*, *Taiyuan University of Science and Technology*, *Taiyuan* 030024, *China*;
4. *State Key Laboratory of Pollution Control and Resources Reuse*, *College of Environmental Science and Engineering*, *Tongji University*, *Shanghai* 200092, *China*;
5. *University of Chinese Academy of Sciences*, *Beijing* 100049, *China*)

Abstract: In recent years, numerous single-atom catalysts (SACs) have been synthesized to activate persulfate (PS) by a non-radical pathway because of its high selectivity, and activity for the catalyst. Metal-nitrogen-carbon (M-N_x-C) has been identified as the key active site in SACs. Although methods for preparing SACs have been extensively reported, a systematic summary of the direct construction of M-N_x-C, especially unconventional metal-nitrogen-carbon (UM-N_x-C, $x \neq 4$), on SACs for PS non-radical activation has still not been reported. The role of the M-N_x-C active sites on PS non-radical activation is discussed and methods for the formation of M-N_x-C and UM-N_x-C active sites in SACs and the effect of catalyst carriers such as carbon nitride (g-C_3N_4), MOFs, COFs, and other carbon materials are reviewed. Direct and indirect methods, especially for UM-N_x-C active site formation, are also elaborated. Factors affecting the formation of a M-N_x-C active site on SACs are also discussed. Prospects for the use of M-N_x-C active sites for the non-radical activation of PS by SACs to remove organic contaminants from wastewater are evaluated.

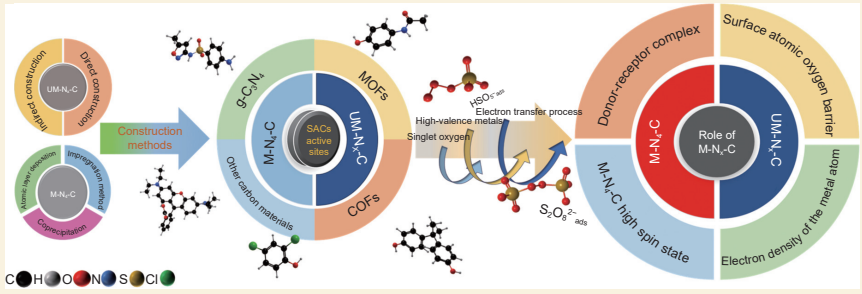

Key words: Single-atom catalysts; Persulfate; Non-radical pathway; Unconventional metal-nitrogen-carbon active site; Organic contaminants

1 Introduction

In recent years, a large amount of wastewater has been discharged with the development of the chemical industry. The wastewater produced from the chemical manufacturing processes process contains a lot of organic contaminants, which are difficult to remove through traditional wastewater treatment technology. The chemical wastewater usually contains phenolic compounds, halogenated hydrocarbons, organic pesticides, hydrocarbons, and endocrine disruptors. These contaminants are carcinogenic, teratogenic, mutagenic, and toxic, and would cause irreversible harm to humans[1–3]. Those refractory organics usually have a stable chemical structure, and the traditional wastewater treatment technologies such as coagulation, adsorption, precipitation, membrane separation are difficult to remove them. In recent years, advanced oxidation processes (AOPs) have been widely used to treat refractory organic contaminants in wastewater[4]. Activated persulfate (PS), as one of the AOPs, is widely used to oxidize refractory organic contaminants in

Received: January 19, 2025
Revised: March 13, 2025
Accepted: March 13, 2025
DOI: 10.1016/S1872-5805(25)60978-4
CSTR: 32158.14.S1872-5805(25)60978-4

wastewater, The sulfate radical ($SO_4^{\cdot-}$) produced by PS activation has a wider pH range, better reaction activity, and a longer half-time than that of hydroxyl radicals (·OH)[5–6]. PS mainly consists of peroxymonosulfate (PMS) and perdisulfate (PDS), which have different characteristics due to the asymmetric structure of PMS. Compared with PDS, PMS has an asymmetric molecular structure, shorter O—O bond length (1.453 π), positive peroxy bond, higher activity, and is easier to activate[7].

PS can be activated using different methods, such as heating, alkali, ultraviolet (UV) light, ultrasound, and other physical methods[8–9]. Meanwhile, incorporating transition metals (including Fe/Co/Mn/Cu/Ce/Ni/Zn) onto metal oxides or activated carbon to form effective heterogeneous catalysts has also been used for PMS activation. However, impurities in complex wastewater, such as salinity wastewater, would consume the free radicals that are highly reactive species with unpaired electrons, mainly ·OH and $SO_4^{\cdot-}$[10–14]. Cl^- would react with ·OH and $SO_4^{\cdot-}$ to form radicals with lower oxidizing state (Eqs. (1-4))[15].

$$SO_4^{\cdot-}+Cl^- \rightarrow SO_4^{2-}+Cl\cdot \quad (1)$$

$$\cdot OH + Cl^- \rightarrow HOCl^{\cdot-} \quad (2)$$

$$H^+ + HOCl\cdot^- \rightarrow Cl\cdot + H_2O \quad (3)$$

$$Cl^- + HSO_5^- \rightarrow SO_4^{2-} + HOCl \quad (4)$$

There are several non-radical pathways for the oxidation of organic pollutants, in which organic contaminants are oxidized by intermediates with high oxidizability rather than radicals. The intermediates with high oxidizability include singlet oxygen ($^1O_2$) oxidation, electron transfer process (ETP), and high-valent metal-oxo species (HVMO). Compared with radical oxidation, non-radical oxidation has significant differences in the oxidation mechanisms, oxidation-reduction potential (relatively mild), activation pathway, and reaction region (surface region)[16–20]. The degradation of organic contaminants by non-radical oxidation has several advantages. Non-radical oxidation has high catalytic activity in a wide range of pH values. Du et al.[21] found that single-atom iron catalysts exhibit high catalytic activity over a wide pH range of 5-9 during the activation of PS. The non-radical oxidation degradation process of organic pollutants is not affected by the presence of inorganic anions in wastewater, and the presence of inorganic anions facilitates the degradation of contaminants. In addition, the non-radical oxidation of organic contaminants in wastewater is not affected by background organic matter in wastewater, such as humic acids[22]. For example, a low concentration of Cl^- is beneficial in promoting the degradation of contaminants, and non-radical oxidation could also significantly reduce the production of toxic by-products[23]. Chloride ions are usually oxidized to form Cl_2 and HOCl in a non-radical oxidation system dominated by $^1O_2$, and the substances formed contribute to the degradation of organic contaminants[24–25]. The non-radical oxidation process can avoid the inefficient consumption of PMS, thus improving its utilization efficiency (stoichiometric efficiency)[26]. These characteristics indicate that non-radical catalytic oxidation has promising applications in pollution control.

Single-atom catalysts (SACs) have attracted considerable attention because of their maximum atomic availability, unique activated sites, and high activity and selectivity in various catalytic reactions[27]. SACs are superior to homogeneous and heterogeneous catalysts and have great application potential in advanced oxidation processes. SACs have been widely used to activate persulfate to degrade organic contaminants in wastewater, improving atom and persulfate utilization efficiency. Miao et al.[28] prepared g-C_3N_4 doped with metal and a Fe-SAC using g-C_3N_4 as the carrier. It was found that Fe-SAC activated PS can improve atom utilization efficiency and persulfate utilization efficiency. The report also pointed out that the complete removal of contaminants by Fe-SAC-activated PS is mainly achieved through the non-radical pathway.

In this work, we outlined the generation and development of the active sites of SACs, usually formed by constructing metal-N_x-C (M-N_x-C) active sites on carbon materials. The M-N_x-C active sites with different N-coordination numbers in SACs have different

roles and construction methods. Several reviews have systematically introduced the applications of SACs to activate persulfate[4,29]. Still, there is been little systematic introduction to designing M-N_4-C active sites and unconventional M-N_x-C (x≠4) (UM-N_x-C) active sites to activate PS and produce non-radical degradation of organic pollutants. In addition, the direct and indirect construction methods of the UM-N_x-C active sites in the SACs and the important factors affecting the construction of the UM-N_x-C active sites are systematically introduced in this work. This review would be helpful for deepening the understanding of the PS activation by the M-N_x-C active sites on the SACs, and provide some enlightenment for the better design of the UM-N_x-C active sites on the SACs.

2 Non-radical pathway mechanism

2.1 Singlet oxygen oxidation

Singlet oxygen ($^1O_2$) is a reactive oxygen species that differs from free radicals. It has a high oxidation-reduction potential and can oxidize organic substrate into smaller intermediate products, which can be converted into CO_2 and H_2O. Meanwhile, $^1O_2$ is a highly selective oxidant that interacts with unconventional organic compounds by electrophilic addition and electron extraction[30]. Typically, in SACs/PS, $^1O_2$ can be generated through various pathways (Fig. 1a), including PS self-decomposition, recombination of $O_2^{\cdot-}$, and the interaction between the catalyst and PS[31–32]. The concentration of $^1O_2$ is affected by several factors including the concentrations of HSO_5^- and $O_2^{\cdot-}$[28,33] (Eqs. (5-7)).

$$HSO_5^- \rightarrow SO_5^{\cdot-} + H^+ + e^- \quad (5)$$

$$SO_5^{\cdot-} + SO_5^{\cdot-} \rightarrow S_2O_8^{2-} + {}^1O_2 \quad (6)$$

$$SO_5^{\cdot-} + SO_5^{\cdot-} \rightarrow 2SO_4^{2-} + {}^1O_2 \quad (7)$$

During the degradation of organic contaminants using SACs to activate PS, the organic contaminants are usually enriched on the surface of SACs, and PMS is activated by the interaction between a single atom with the surrounding coordination atom, this contributes to the production of $^1O_2$ by activating PMS. It was found that the Fe-N_x-C active site in Fe-SAC[34], the Cu-N_x-C active site in Cu-SAC[24], and the Co-N_x-C active site in Co-SAC[35] could effectively activate PS to produce $^1O_2$. However, the $^1O_2$ has a relatively short life and is not as strong as radicals of $SO_4^{\cdot-}$ and ·OH for the reduction of wastewater COD or TOC[36]. Therefore, the content of $^1O_2$ can be increased by increasing the PS, H_2O_2, and other oxidants in the system. A summary of the reported non-radical pathways for PS activation with single-atom catalysts is provided in Table 1.

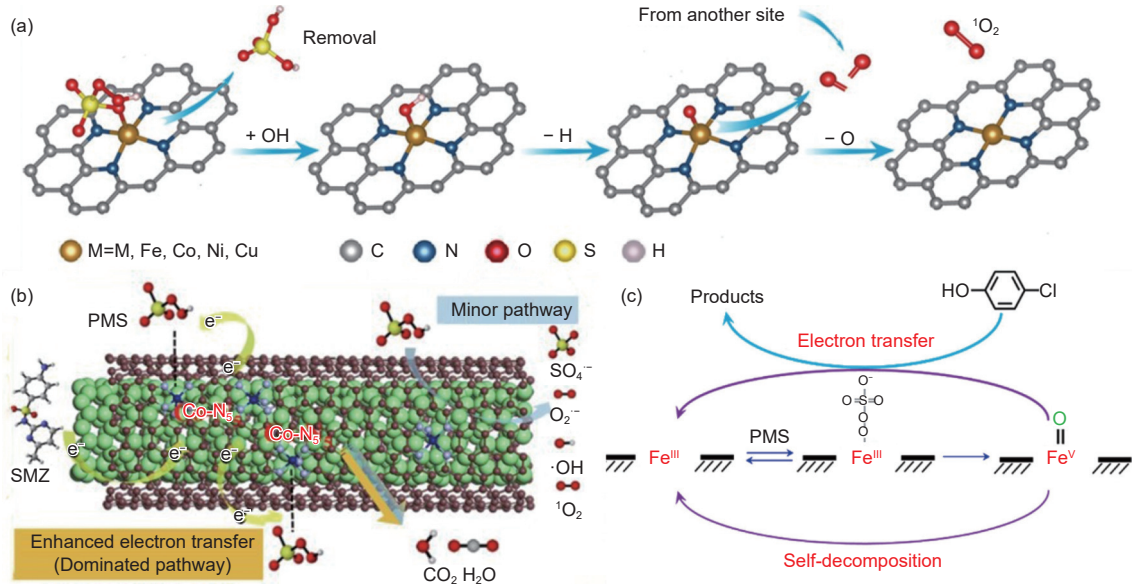

Fig. 1 Different pathways for PMS activation: (a) $^1O_2$ (Reprinted with permission, Copyright 2021, Wiley)[60]. (b) Electron transfer (Reprinted with permission, Copyright 2022, Elsevier)[61] and (c) high-valent metal (Reprinted with permission, Copyright 2018, American Chemical Society)[30]

2.2 Mediated electron transfer

The mediated electron transfer process is one of the non-radical pathways in the activation of PS by SACs (Fig. 1b). Quenching experiments usually confirm this to eliminate the effects of radicals and $^1O_2$. The contaminant degradation through the mediated electron transfer process is that organic contaminants adsorb on the M-N_x-C active sites in SACs to form a "donor-receptor complex" with PS, which enables electron transfer from co-adsorbed organics (electron donors) to PS (electron receptors) and leads to a direct attack on organics[20,37–39]. It has been found that many factors influence the electron transfer process, including the concentration of contaminants, the content of PMS/PDS in the system, and the coordination configuration of different metal centers[37,40–41].

Usually, the sp^2 hybrid carbon network affects the electronic configuration of PS, weakens the O—O bond and forms metastable complexes (the active state of PS)[42–44]. The existence of organic contaminants enhances PS decomposition. The electron donor-mediator (SACs)-receptor ternary system was formed when the organic contaminants were in contact with activated PS molecules. With the help of SACs, the activated PS can degrade pollutants through non-radical generation by double-electron conduction.

2.3 High-valence metal oxidation

High-valent metal-oxo species (HVMO) have been identified as the reactive-active species[45] in PS/SAC systems, which attack organics mainly through electron transfer and oxygen transfer[46–47]. Their oxidation ability primarily comes from 2 ways: (1) the direct oxidation of high valence metal and (2) the indirect oxidation ability transfer from PS. Peng et al.[48] and Li et al.[49] found that the formation of high valence metal is affected by the content of pyridine N rather than environmental pH. A higher pyridine N content would lead to higher valence metal on the SACs. Li et al.[30] successfully doped Fe (III) into g-C_3N_4, a mechanism for the activation of PMS by high-valent iron-oxo species for organic contaminants degradation was proposed (Eqs. (8, 9)): PMS first binds to the Fe(III) to generate Fe(V)=O, then reacts effectively with the pollutant (Fig. 1c).

Table 1 Examples of a non-radical pathway in the activation of PS by a single-atom catalyst

SACs carriers	Catalysts	PMS/PDS	Non-radical pathways	Contaminants (concentration)	Degradation complete /(min)	Refs.
ZIF-8	Fe-SACs (0.15 g/L)	PMS (0.4 g/L)	ETP	BPA (20 mg/L)	20	[37]
g-C_3N_4	Fe-SACs (0.1 g/L)	PMS (0.4 g/L)	ETP	O-phenyl phenol (10 mg/L)	40	[51]
g-C_3N_4	Zn-SACs (0.1 g/L)	PDS (2 mM)	ETP	BPA (100 μM)	35	[52]
Waste biosorbent	Cu-SACs (0.1 g/L)	PMS (0.4 g/L)	ETP	BPA (20 mg/L)	30	[53]
Polymeric carbon nitride	Co-SACs (0.2 g/L)	PMS (0.2 g/L)	$^1O_2$	Tetracycline (20 mg/L)	After 60	[54]
ZIF-8	Fe-SACs (0.1 g/L)	PMS (0.2 g/L)	$^1O_2$	Sulfasalazine (20 μM)	After 30	[55]
ZIF-8	Cu-SACs (0.2 g/L)	PMS (0.2 g/L)	$^1O_2$	Sulfamethoxazole (18 mg/L)	65	[56]
Biochar	Fe-SACs (0.1 g/L)	PMS (0.3 g/L)	HVMO	Paracetamol (10 mg/L)	60	[48]
ZIF-8	Fe-SACs (0.15 g/L)	PMS (0.4 g/L)	HVMO	BPA (20 mg/L)	30	[49]
Biochar	Co-SACs (0.1 g/L)	PMS (0.2 g/L)	ETP/$^1O_2$	CQP (10 mg/L)	30	[57]
Biochar	Co-SACs (0.1 g/L)	PMS (0.6 g/L)	ETP	APAP (10 mg/L)	11	[58]
Expanded graphite	Co-SACs (0.2 g/L)	PMS (0.2 g/L)	ETP/$^1O_2$	LEVO (24 mg/L)	60	[59]

Note: M: mol L^{-1}

$$Fe(III) + SHO_5^- \rightarrow Fe(V) = O + SO_4^{2-} + H^+ \quad (8)$$

$$Fe(V) = O + organics \rightarrow Fe(III) + products \quad (9)$$

The binding energy of Co with PMS is higher than that of N or C, so PMS is more likely to be adsorbed onto the Co atom of the Co-N_x-C active center to form a more stable PMS-Co-N_x-C structure[50]. Co (II) at the Co-N_x-C active site acts as an electron donor during the PMS activation to form $SO_4^{\cdot-}$ and high-valent Co (IV)=O. Subsequently, the high-valent Co (IV)=O with high activity can oxidize organics on the catalyst surface to form intermediates and small molecules. The specific reaction equations are as follows (Eqs. (10, 12)):

$$HSO_5^- + HSO_5^- \rightarrow 2SO_4^{2-} + 2H^+ + {}^1O_2 \quad (10)$$

$$Co(II) + HSO_5^- \rightarrow Co(IV) = O + SO_4^{2-} + H^+ \quad (11)$$

$$Co(IV) = O + organics \rightarrow Co(III) + products \quad (12)$$

3 Function of M-N_x-C active sites

3.1 The role of the M-N_4-C active sites

The M-N_4-C active site configuration on the SACs is usually composed of one metal atom covalently linked to four pyridine N or pyrrole N atoms, in which the abundant d-orbital electrons of transition metals can significantly modulate the local electronic structure through the strong electron metal-carrier interaction. As their stable active sites, M-N_4-C active sites have been widely used to activate PS to generate non-radical pathways for efficient degradation of organic contaminants[60,62–66].

Metal atoms are the main active centers in the process of PS activation by SACs. At the same time, the coordination environment also plays an essential role in regulating SAC activity and the PS activation pathway. The reports discovered that the coordination environment can be further optimized by adjusting the coordination number, configuration, and metal spin status[67]. The coordination structure of SACs can be directly affected by changing the coordination ratios of different N-groups (pyridine N, pyrrole N and graphite N) with a single metal atom[68].

For the non-radical activation process of PS on M-N_4-C, PS-M-N_4-C as an adsorption site for contaminants, contaminants were adsorbed to the active site of M-N_4-C through the "donor-receptor complex" mechanism to form non-radical PS intermediates (Fig. 2). Then, the pollutants were degraded through non-radical pathway ($^1O_2$, ETP, and HVMO) effectively[69]. It is found that M-N_4-C active sites on SACs can adsorb PS to form metal-containing metastable in-

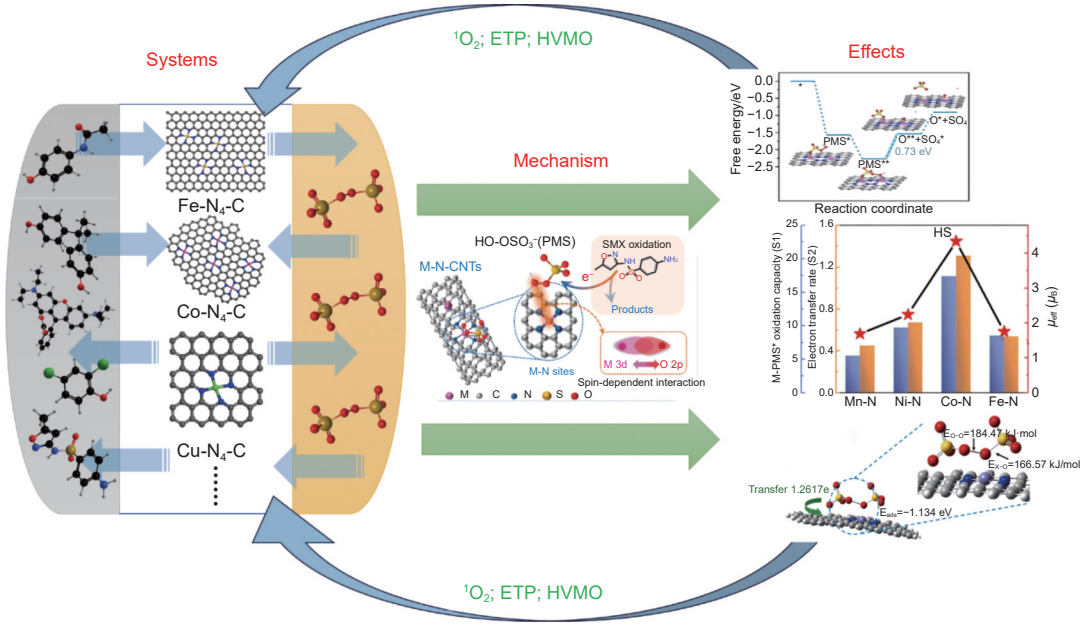

Fig. 2 Mechanism of two effects on pollutant degradation derived from the spin-state change generated by activation of PS at the M-N_4-C active sites on the SACs (Reprinted with permission, Copyright 2021, American Chemical Society) (Reprinted with permission, Copyright 2023, Wiley) (Reprinted with permission, Copyright 2023, Elsevier)[70,83,85–87]

termediates, and the PS can be spontaneously adsorbed on the coordination active sites of M-N_4-C, triggering S—O bond breakage and O—O bond polarization in PS and the selective generation of $^1O_2$[35,39,70]. The calculation results based on density functional theory (DFT) also showed that the degradation of contaminants was mainly achieved on the active site of M-N_4-C, which formed metal-O-O-SO_3^- through the adsorption of PS and reacts with HSO_5^- to form $^1O_2$[39].

In addition, SACs are often used to activate PS to form high-valent metal species through the "donor-receptor complex" mechanism for degradation of organic contaminants. Jiang et al.[71] and Wang et al.[72] proposed that during non-radical oxidation, single atom Fe (III) is converted to Fe (V) by PDS double-electron extraction after coordination with pyridine N atom, Fe (V) may be an intermediate oxidant for the removal of contaminants. Further studies found that in Co-SAC, the active site of Co-SAC elongates its O—H and O—O bonds and spontaneously dissociates to H^+, and SO_4^{2-} by adsorption and activation of PS, O atoms coordinate with the Co atoms to form a high valence Co═O structure[39].

On the other hand, SACs are also often used to activate the PS generation electron transfer pathway for the degradation of organic contaminants through the "donor-receptor complex" mechanism. The application of ETP in the degradation of enrofloxacin (ENR) in the Mn-SAC/PMS system was proposed by designing Mn-SAC for the degradation of ENR by activated PMS. Firstly, the O—O bond of PMS polarizes the original Mn (III)-N_4-C active site position to form Mn (IV)-N_4 species, and then PMS is further adsorbed by Mn (IV)-N_4-C active sites to form Mn (IV)-$OOSO_3^-$complex, the electron transfer from ENR to Mn-SAC is promoted. Then, Mn (IV)-$OOSO_3^-$ will be further attacked by internal nucleophiles to form $O_2^{\cdot-}$/$^1O_2$ and surface Mn (III). Mn-SAC acts as an electron shuttling. Through the redox cycle of Mn (III)/Mn (IV) on the surface, the electrons are transferred from ENR to PMS, and the effective degradation of contaminants is realized[73].

Research has shown that in the design of SACs, the coordination state between metal atoms and nitrogen atoms has a significant impact on the spin state of the metal atoms. The spin state of metal atoms means the arrangement of electron spins within the metal atom. Typically, in M-N_x-C activate sites under weaker crystal fields, electrons tend to spread across different orbitals, maintaining the state of unpaired electrons as far as possible. This leads to a higher total spin quantum number, known as the high-spin state (such as the high activity of Mn-N_5 was discerned to be the formation of higher-spin-state N_5Mn (IV)=O species)[74–76].

The larger spin-state values of M—N enhance catalytic activity for PMS activation, attributed to the spatial electronic configurations of the transition metal d orbitals. Typically, the e_g orbital of transition metals engages in σ-bonding with oxygen-containing species by overlapping with the O 2p orbitals, which influences the bonding strength and electron transfer rates, thereby affecting the catalytic activity for PMS activation. The high-spin state of M—N sites, with a large magnetic moment, favors the coupling of oxygen-containing adsorbates on metal sites and enhances the transfer of spin-oriented electrons. This, in turn, promotes PMS adsorption, strengthens the oxidation potential of the intermediates, and accelerates electron transfer, resulting in improved catalytic activity for PMS activation and organic pollutant oxidation[77–82]. Miao et al.[83] and Zhang et al.[84] proposed that the spin state of Fe in Fe-N_4-C active sites determines the generation of reactive species and electron transfer pathways in the Fe-N_4-C/PMS system. The relative content of high-spin species (Fe (II) and Fe (III)) promoted catalytic performance. Fe (II) in the active site of Fe-N_4-C activates PMS by a single-electron transfer, forming sulfate and hydroxyl radicals and the Fe (III) in the active site of Fe-N_4-C is more inclined to produce high-valent iron oxides with lower free energy.

In summary, the coordination environment plays an important role in regulating SAC activity and activating the PS pathway. By changing the coordination

ratio of the N atom with a single metal atom, the active sites of PS activation in SACs can be affected, ultimately achieving the degradation of organic pollutants through the "donor-receptor complex" mechanism. Additionally, the formation of high-spin state coordination structures enables the effective transfer of electrons from organics to the metal site through a lower energy barrier, thereby achieving the degradation of organic compounds.

3.2 The role of the UM-N_x-C active sites

It is widely believed that the UM-N_x-C active sites have a higher activity on PS activation than M-N_4-C active sites on the SACs with a similar non-radical pathway.

However, there are two different mechanisms of UM-N_x-C active sites for improving the activity of SACs on PS activation. Firstly, the unconventional coordination of UM-N_x-C active sites greatly affects the electron density of the metal atom, enhancing the interaction between metal centers and PS in SACs and facilitating the removal of organic contaminants by PS[88–90]. Different UM-N_x-C active sites have different activation properties of PS, and it is generally believed that the unconventional monatomic sites of transition metals have higher activity. Among the UM-N_x-C (M = Fe, Co, Cu, Mn, etc.) active sites, it is reported that a lower coordination number of Co-N_3-C active site leads to higher adsorption-free energy and a unique electron transfer mechanism, which makes the electron density of Co-N_3-C active site higher than that of Co-N_4-C active site and enhances the interaction between Co and PS in SACs[89,91–92]. Interestingly, the enhancement mechanism of lower coordination numbers was also found in Zn-SACs. The unconventional Zn-N_3-C active sites promote electron delocalization and decrease the average valence state of Zn in the mixed coordination Zn-N_x-C active sites, which benefits the interaction between Zn-SACs and PS. Xin et al. proposed high-loading and low-valence Zn-SACs to obtain a fast Fenton-like catalyst with the formation of Zn-SAC/PS complex and efficiently reducing contaminants through a strong direct electron transfer pathway[52]. It has also been reported that the asymmetric structure of the UM-N_x-C/PS system exhibits obvious selectivity, anti-interference ability, and durability for contaminant removal in the complex matrix. This may be due to the fact that the energy barrier of PS dissociation on UM-N_x-C active sites is much lower than that of M-N_4-C active sites[29,93]. Secondly, the enhancement of the PS activation by UM-N_x-C active sites can also be realized by decreasing the surface atomic oxygen barrier by affecting the O—O bond energy in PS. It has been found that the UM-N_x-C (M = Fe or Mn) active site has a higher activity to weaken the O—O bond energy in PS and cause it to break, reducing the surface atomic oxygen barrier and producing abundant $^1O_2$ oxidizing contaminants and their intermediates[94–95]. Song et al.[96] found that Fe-SAC with the Fe-N_5-C active site had a greater effect on the O—O bond energy in PMS compared to the Fe-N_4-C active site, which can efficiently degrade acyclovir by generating $^1O_2$ and Fe (IV)=O non-radical pathways. Furthermore, the UM-N_x-C active site could produce high-valent metal-oxo species besides $^1O_2$ for pollutant degradation (Fig. 3).

4 Construction methods and materials of M-N_x-C

4.1 Construction of carrier materials for M-N_4-C

4.1.1 Carbon nitride (g-C_3N_4)

Two-dimensional (2D) graphite carbonitride (g-C_3N_4) consists of three layered hexagonal units and forms a sheet π-π conjugate structure consisting of sp^2C and sp^2N[97]. The abundant nitrogen atoms in g-C_3N_4 facilitate the anchoring of individual metal atoms through the effective coordination between the empty orbitals of metal atoms and the lone pair electrons of nitrogen. Meanwhile, the folded space of g-C_3N_4 benefits the stabilization of metallic single atoms. Therefore, g-C_3N_4 may serve as a promising 2D carbon structure for constructing SACs[98]. It was found that SACs using g-C_3N_4 as carbon carriers had high specific surface area and abundant pore structure (Fig. 4a). It has a positive effect on the PS activation to form high-valent metal-oxo species and $^1O_2$[99]. Al-

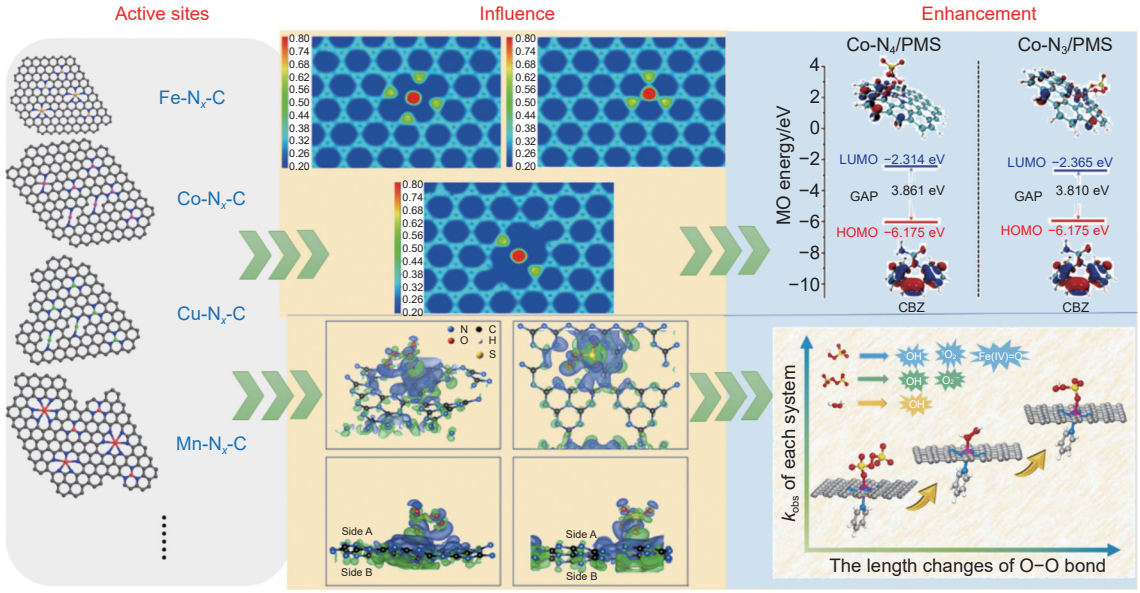

Fig. 3 Enhancement of non-radical pathway by the UM-N$_x$-C active sites (Reprinted with permission, Copyright 2022, Wiley) (Reprinted with permission, Copyright 2021, Elsevier) (Reprinted with permission, Copyright 2023, Elsevier) (Reprinted with permission, Copyright 2023, Elsevier)[51,90–91,96]

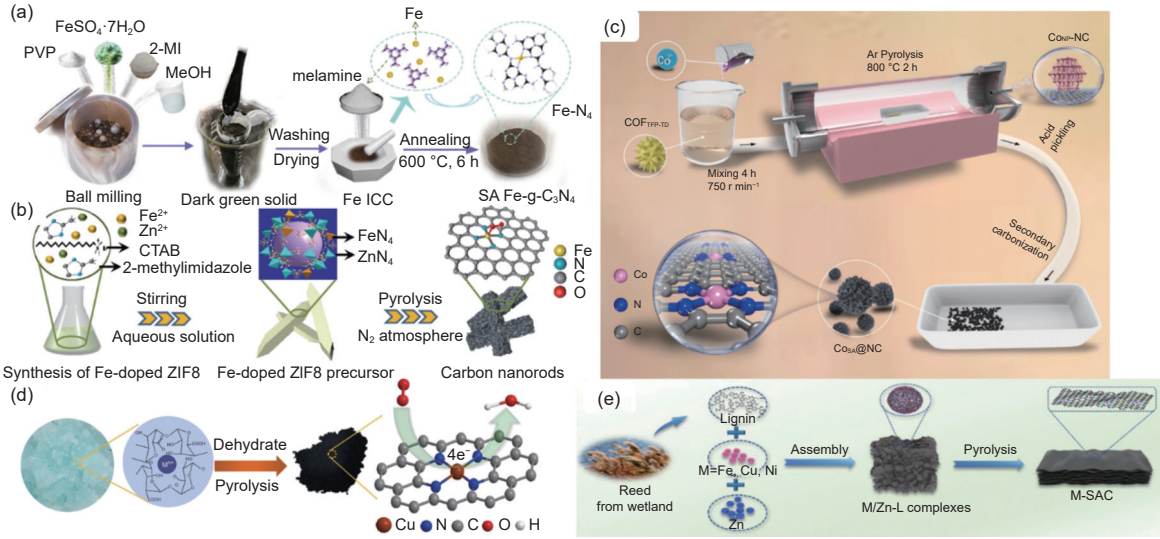

Fig. 4 SACs prepared with different carbon carriers: (a) G-C$_3$N$_4$ (Reprinted with permission, Copyright 2022, Elsevier)[128], (b) MOFs (Reprinted with permission, Copyright 2021, American Chemical Society)[129], (c) COFs (Reprinted with permission, Copyright 2024, Elsevier)[130], (d) Biomass carbon (Reprinted with permission, Copyright 2021, American Chemical Society)[131] and (e) carbon nanotubes (Reprinted with permission, Copyright 2022, Elsevier)[132]

though there are abundant N sources in carbon nitride, adding N sources can enhance the coordination of carbon nitride and metal atoms to form SACs. Liu et al.[100] used dicyandiamide as N source to strengthen the coordination of Fe on g-C$_3$N$_4$. The content of Fe can reach 2.03%, and the content of N element in SACs can reach 38.2%. In addition, attempts to anchor other metals onto g-C$_3$N$_4$ carriers to construct SACs have been investigated[101–104]. There are a large number of studies about SACs using g-C$_3$N$_4$ carriers. Wu et al.[105] and Gao et al.[60] proposed the performance order of different SACs using g-C$_3$N$_4$ as a carrier Fe-SAC > Co-SAC > Mn-SAC > Ni-SAC > Cu-SAC. Carbon nitride has become a frequently used carbon material for preparing SACs for PS activation. In addition, the physical appearance of g-C$_3$N$_4$ also affects its activity. Carbon nitride is easy to crimp during calcination, and the crimp structure is not conducive to sufficient contact and reaction between a single atom site and PS. Therefore, some studies have

been done to control carbon nitride morphology to help form more M-N_4-C active sites. Liu et al.[100] prepared anti-curling g-C_3N_4 SACs with hemin as a metal source. As the iron in hemin is difficult to aggregate during pyrolysis[106–107], the curling of g-C_3N_4 was inhibited by using hemin as a precursor. The anti-curling of g-C_3N_4 was beneficial to forming the active site of M-N_4-C.

4.1.2 Carbon materials derived from MOFs

Metal-organic frameworks (MOFs) are unique porous crystal materials composed of metal ions/clusters and organic linkers. Because of its structural diversity, adjustable function, and high specific surface area, different MOF-based SACs can be well developed, forming unconventional coordinating metal sites from metal nodes and metal junctions[108]. In recent years, MOFs with ultra-fine porosity, assembled from functional organic linkers and metal nodes, have attracted much attention as precursors for preparing porous SACs. It has also become an important precursor material for the construction of SACs[109–111].

Because of its simplicity, the zeolite imidazole skeleton (ZIF-8) is used as a MOF precursor for SACs (Fig. 4b). ZIF-8 can be used as a carbon material precursor. After the pyrolysis at 900 °C, Zn was removed to form a carbon carrier with abundant defects and microporous structure, which is a good carrier for preparing SACs[112]. The removal of Zn atoms by high temperature is likely to produce more defect sites on the carrier to increase the specific surface area of the carrier. It has been found that ZIF-8 can be synthesized by using methanol, 2-methylimidazole, and Zn $(NO_3)_2\cdot 6H_2O$ as precursors of SACs. Then, the Zn atoms are removed by high-temperature pyrolysis, which destroys the original structure of the carrier and forms more defects, making it easier to synthesize M-N_4-C or UM-N_x-C active sites.[113–115].

4.1.3 Carbon materials derived from COFs

Covalent organic frameworks (COFs) are a kind of crystalline organic polymers with porous, highly ordered, and tunable structures[116]. Recently, COFs have been regarded as a promising 2D and 3D crystalline polymer precursor for preparing SACs. COF-based SACs are typically prepared by introducing a single metal atom, utilizing the coordination in the organic linker and the pore size limiting effect of COF framework, and finally forming SACs after pyrolysis at high temperatures (Fig. 4c). Compared with MOFs, COF exhibits great stability in organic solvents or highly acidic and alkaline solutions, it also has the advantages of porous structure, custom function, and high metal loading. SACs based on COFs have become important catalysts for efficient catalytic reactions[117–120]. Peng et al. successfully introduced a single Cu atom and electron donor group into COFs based on ketamine and successfully synthesized Cu-SAC with COFs as carriers. It was found that the introduction of individual metal atoms increases the electron density at the active center, and electron-donating groups accelerate the transfer of photogenerated carriers and improve the PMS adsorption to the material, thus significantly improving the catalytic activity. After five consecutive recycles, Cu-SAC can remove more than 92% of the contaminants with a high content[121].

Because of the similar structure between MOFs and COFs, COFs are often used to combine MOFs to prepare complex SACs. Liu et al.[122] prepared a core-shell SAC using a precursor with a COF (TP-BPY-COF) as the shell and a MOF (ZIF-67) as the core. The thin COF shell not only prevented the collapse and aggregation of ZIF-67 but also facilitated mesopore formation for mass transport and improved graphitization for enhanced conductivity. The SAC had M-N_4-C atoms together with metal nanoparticles embedded in carbon, which enables catalyzing the oxygen reduction reaction with high activity and excellent stability. This SAC derived from the MOF/COF composite may be used to activate PS to degrade organic contaminants in wastewater.

4.1.4 Other carbon materials

SACs show great application potential for the oxidation process. It is important to find high-performance, low-cost materials as precursors of SACs. Biochar, carbon fibers, and other carbon materials are

also popular materials for preparing SACs besides g-C_3N_4, MOF-derived carbons, and COF-derived carbons. SACs can be prepared by using waste biosorbents[53], iron-rich enteromorpha[48], wastewater sludge[35], and biomass to activate PS for pollutant degradation[123].

The easy availability of carbonaceous compounds could significantly reduce the preparation cost such as common lignin, waste paper-derived active carbon, and other biomass materials (Fig. 4d). Yang et al.[40] modified the Co/Zn-lignin complex through N doping, and the construction of Co-SACs was realized after a high-temperature calcination treatment under the protection of the N_2 atmosphere. In addition, Qian et al.[124] anchored metal atoms to waste paper-derived active carbon materials, and SAC containing the active site of UM-N_x-C was prepared. There are also many reports on the construction of SACs through calcining carbonaceous compounds. Sodium citrate[89] and tetrahydrofuran[125] were the precursors to easily obtain Co-SAC and Cu-SAC with an N-source addition and calcination. Therefore, the carbon carriers for preparing SACs are abundant and easy to get. SACs can be prepared from carbonaceous materials and carbonaceous organic compounds in a relatively simple process, and it is easier to synthesize complex and diverse active sites.

The construction methods of SACs from carbon fibers are becoming more and more mature, but there are not many cases of using carbon fiber-based SACs for PS activation to degrade organic contaminants in wastewater (Fig. 4e). The porous and hetero-atom modifications are usually used for carbon fiber pretreatment to optimize the coordination environment and electronic structure of isolated metal atoms and better construct M-N_x-C active sites[126–127]. Duan et al.[85] found that a higher content of pyridine N created more defects for metal coordination and the anchoring of metals on the SAC also promotes N-doping, which ensures the atomic dispersion of metals on the carbon surface.

4.2 Construction of M-N_4-C active sites

The M-N_4-C active site is the key active site of SACs, mainly constructed by anchoring metal atoms on the carbon carrier containing N. The catalytic performance of M-N_4-C active sites generally depends on the coordination environments of the central metal atoms[133]. The metal in the M-N_x-C active site is mainly composed of multivalent transition metals such as Fe, Co, Cu and Mn. As the stable structure and facile construction methods, the construction of the M-N_4-C active site for PS activation is the research hotspot[83,89,125]. Besides usual transition metals, it has been found that Zn and Ni can be used as the new transition metal atoms to prepare the active sites of M-N_4-C on the SACs, which can activate PS to produce a non-radical pathway for the effective degradation of organic contaminants[134]. The main factors affecting the construction of M-N_4-C active sites include carriers, immobilization methods, pyrolysis conditions, and so on.

It is well known that preparing SACs with high metal loading and minimal agglomeration is challenging. The construction of M-N4-C requires more accurate metal anchoring and homogeneous metal dispersion. To prevent the formation of excessive clusters and nanoparticles during the preparation of SACs, more and more innovative methods have been employed in recent years. Among these, atomic layer deposition (ALD) creates metal vacancies by anchoring and dispersing metal atoms strongly, so facilitating the formation of SACs. The coprecipitation and impregnation methods typically control the metal loading, and acid washing on the catalyst before and after the pyrolysis reaction, effectively prevents the excessive formation of clusters and nanoparticles[135].

4.2.1 Atomic layer deposition

Atomic layer deposition (ALD), a technique that allows the controllable synthesis of materials at atomic scale, began in the late 1990s and early 2000s[136]. The method is a cyclic process based on continuous self-limiting molecular surface reactions between gaseous chemical precursors and solid substrate surfaces, which has been used to design and prepare SACs with atomic-level control[137]. ALD can precisely control the deposition of individual atoms and

nano-clusters, allowing precise control of atomic layer thickness at 100 nm or single-layer levels. Recent research discovered that controlling the number of ALD cycles and the deposition temperatures can increase the metal load on the SACs. In addition, the size of SACs can be controlled by ALD, and SACs prepared by ALD have high stability[136]. SACs obtained through ALD have extremely high atomic utilization efficiency[138–139]. Based on this, Li et al. used the ALD method to prepare highly loaded Pt atoms on nitrogen-doped carbon nanoplates[140] (Fig. 5a).

In addition, Stambula et al. have prepared isolated single Pt atom catalysts on N-doped graphene nanosheets (NGNs) by ALD. They found that the size of Pt catalysts on the NGNs was controlled by adjusting the number of ALD cycles. Regardless of applying 50, 100 or 150 ALD cycles, Pt-SAC can be observed[141]. In addition, Wang et al. also synthesized Fe-SAC successfully by the ALD method and found that the photocatalysis experiment demonstrated that TiO_2 nanoparticles, deposited with two cycles of Fe ALD, showed the highest activity and had a more than 6-fold photocatalytic activity enhancement over pure TiO_2 for the degradation of contaminants[142].

4.2.2 Coprecipitation

In a typical coprecipitation process, there are 2 or more cations in the solution as a homogeneous phase, a homogeneous precipitation of various metal components can be obtained after adding a precipitator and a precipitation reaction. Coprecipitation is an important method for preparing composite oxide ultrafine powders containing two or more metals[143–144]. Owing to its ease of mass production and operation, it has been widely used for metallic oxide preparation while the coprecipitation process inevitably leads to metal atoms being buried within the bulk of the material, which limits the accessibility of these metal atoms in the catalysis process[145].

There are many cases of preparing SACs by the coprecipitation method. Zeng et al. have successfully incorporated ruthenium and copper single atoms into polymeric carbon nitride (PCN) through a simple preassembly-co-precipitation-pyrolysis process. This method led to the formation of atomically dispersed Ru-N_4 and Cu-N_3 active sites[146] (Fig. 5b). Shi et al.[147] used a series of CeO_2-TiO_2 mixed oxides as supports with various Ce/Ti molar ratios synthesized by a modified coprecipitation method. The corresponding Pt-SAC was prepared by an electroless deposition method. Meanwhile, Yi et al.[148] employed a single-atom Pt and an ionic liquid to prepare the Pt-SAC for coprecipitation with ReO_4^- salt. The con-

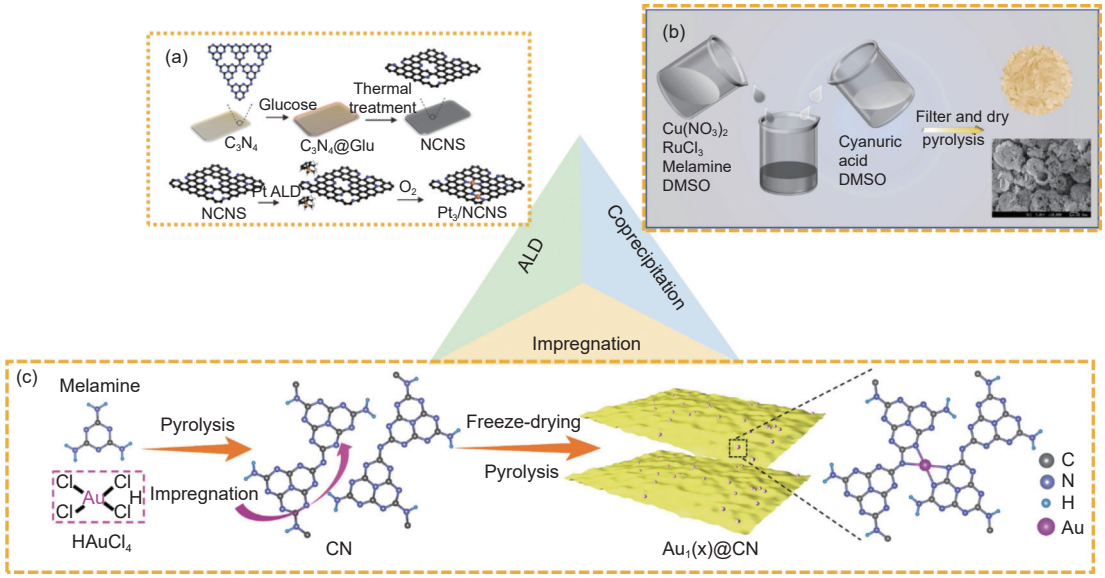

Fig. 5 (a) High-loading Pt single atom on N-doped carbon nanoplates (PT-1/NCNS) achieved by ALD method (Reprinted with permission, Copyright 2021, Wiley)[140]. (b) Ru and Cu loaded onto carbon nitride by the coprecipitation method (Reprinted with permission, Copyright 2022, Elsevier)[146]. (c) Au-SAC prepared by the impregnation method on porous C_3N_4 nanosheet loaded with Au (Reprinted with permission, Copyright 2024, Elsevier)[149]

struction method is simple, but the metal load is not very high because the metal atoms are easily covered.

4.2.3 Impregnation method

Some advanced impregnation methods have been proposed to regulate the M-N_4-C active sites more precisely (Fig. 5c). For the impregnation process, a solid or a shaped support is immersed into a metal salt solution and the active metal is attached to the carrier in the form of ions or compounds after separation of the carrier from the residual liquid[135]. Hu et al.[149] used porous C_3N_4 nanosheets as supports to prepare Au single atoms catalyst (Au-SAC) with Au-N_4 active sites via a facile "impregnation + freeze-drying" process. This advanced impregnation method resulted in Au SAC that exhibited efficient and stable performance. Wang et al.[150] proposed a two-step ion exchange method for SAC construction, and transition metal (M = Fe, Co, Ni, Cu) was precisely anchored on ZIF-8 derived carbon carriers to form the M-N_x-C active sites. The SACs obtained by the impregnation method have high metal content and uniform metal dispersion, which is beneficial to forming M-N_x-C active sites to adsorb and activate more PS.

4.3 Construction of UM-N_x-C active sites

It has been revealed that the number of N coordination greatly affects the activity of active sites for PS activation[151–152]. M-N_4-C active sites with a symmetric coordination structure have excellent activity in SACs. However, the adsorption energy of intermediates on the M-N_4-C active site is not always the highest in a PS activation process. Experimental and theoretical studies show that the D-band of metal can move toward the center and exhibit more electronic states by adjusting the microenvironment with a reasonable coordination structure[153]. The difference in charge distribution can be used to regulate the adsorption energy of the intermediate, thus achieving higher activity[154–155]. The M-N_4-C active sites usually have a stable covalent structure, so the number of N atoms can hardly be increased or decreased. Some effective methods have also been proposed to enhance the activity of SACs by regulating the coordination number of M-N_x-C active sites and constructing UM-N_x-C active sites.

The structure of the UM-N_x-C active sites can be obtained by direct or indirect construction. Construction of UM-N_x-C active sites requires a more elaborate process design than M-N_4-C active sites. This paper summarizes the literature on UM-N_x-C and M-N_4-C active sites, as listed in Table 2.

4.3.1 Direct construction method

It was found that the structure defects of the precursors affected the construction of the UM-N_x-C active sites in the direct structure process. In addition, the content of N in SACs also played an important role in the N coordination number of UM-N_x-C active sites. The number increases with the content of the N atoms, especially pyridine N and graphite N, facilitating electron transfer and affecting the electron density around metal atoms. Zhang et al.[156] employed kaolin clay with abundant defect sites as carrier. The layered kaolin clay provides abundant anchoring space for Fe-SAC, which is destroyed by pyrolysis at high temperatures to produce the N vacancy defect sites. The electron structure of the Fe atom was optimized by increasing the N vacancy concentration, and the Fe-N_5-C active site was successfully constructed on Fe-SAC. Wang et al.[157] and Qian et al.[124] have successfully prepared Co-SAC containing Co-N_3-C active sites using hydrogel and nano-biocarbon as precursors. This is mainly owing to the abundant structural defects of the precursor carbon materials. Co atom in the UM-N_x-C active site was bound to pyridine N, which means that pyridine N facilitates the formation of Co-N_3-C active site coordination.

MOF materials were transformed into porous graphene-based carbon materials with a large specific surface area and abundant defect structure. They were treated to prepare SACs containing the active site of UM-N_x-C. The active site of UM-N_x-C was easily formed on the precursor materials with abundant defect sites by binding pyridine N to metal atoms and pyrolysis at high temperatures. The interaction between pyridine N and metal atoms results in a slight decrease in the electron density of the N atom, enabling the N atom more favorably to bond with the M atom and form the UM-N_x-C active site. This method

Table 2 Construction methods of M-N_4-C and UM-N_x-C

	Construction method	Sites	Carriers	Active species	Synthesis method	Loading/%	Ref.
M-N_4-C	Coprecipitation	Fe-N_4-C	ZIF	$^1O_2$	Pyrolysis of $Fe(acac)_3$ encapsulated ZIF-8 in N_2 at 900 °C, 3 h	6.32	[55]
	Coprecipitation	Co-N_4-C	Cobalt-based nanomaterials	$^1O_2$	Pyrolysis of DPA-cnMoS_2 N_2 at 600 °C, 2 h	4.79	[164]
	Impregnation	Cu-N_4-C	Carbon matrixes	$^1O_2$	Pyrolysis of $CuCl_2$ and metallic precursor in N_2 at 550 °C, 1 h and at 950 °C, 1 h	0.33	[132]
	Impregnation	Fe-N_4-C	Fe-imidazole coordination precursor	ETP/$^1O_2$	Pyrolysis of Fe-imidazole coordination precursor in N_2 at 600 °C, 6 h	4.82	[165]
	Coprecipitation	Mn-N_4-C	NCNTs	ETP	Pyrolysis of Mn_{ap}-NCNT in N_2 at 800 °C, 2 h and at 600 °C, 2 h	0.47	[85]
	ALD	Ni-N_4-C	Carbon nitride	High-valent Ni and ETP	Pyrolysis of carbon nitride polymer, at 450 °C, 4 h	3.2	[166]
UM-N_x-C	Directly	Fe-N_3-C	ZIF	$^1O_2$	Pyrolysis of Fe-doped ZIF-8 in Ar at 900 °C, 2 h	0.75	[162]
	Directly	Fe-N_5-C	Nitrogenated carbon	$^1O_2$	Pyrolysis of $FeCl_2$ and dicyandiamide in Ar at 800 °C, 3 h	1.68	[96]
	Directly	Co-N_2-C	ZIF	$^1O_2$	Pyrolysis of Zn/Co-ZIFs in Ar at 800 °C, 3 h	2.26	[90]
	Directly	Cu-N_2-C	ZIF-8	ETP	Pyrolysis of Zn/Cu-ZIF-8 in N_2 at 1000 °C, 2 h	1.57	[167]
	Directly	Co-N_3-C	Biomass carbon	ETP	Pyrolysis of precursors, DCD, and NaOH in N_2 at 1000 °C, 1 h	1.15	[23]
	Indirectly	Mn-N_6-C	ZIF-8	$^1O_2$	Pyrolysis of Z8-Mn@g-C_3N_4 in Ar at 550 °C, 4 h and at 1100 °C, 2 h	0.95	[94]
	Indirectly	Cu-N_3-C	Waste adsorbent-based biochar	ETP	Pyrolysis of mixture in N_2 at 550 °C, 1 h and at 900 °C, 1 h	3.41	[53]
	Indirectly	Co-N_3-C	Active carbon	$^1O_2$	Pyrolysis of WP-COOH in N_2 at 550 °C, 2 h and at 700 °C, 1 h	—	[124]
	Directly	Co-N_3-C	Biomass carbon	ETP	Pyrolysis of mixture in N_2 at 600 °C, 1 h	0.11	[58]

has become widely used for UM-N_x-C active site construction, by which Cu-SAC containing the Cu-N_3-C active sites and the Mn-SAC containing Mn-N_3-C active sites were prepared[158–160].

To construct more UM-N_x-C active sites, several pre-treatments were proposed to create more defects on the carrier, favoring metal atom dispersion and exposure. Li et al.[38] used the template-etching method to remove nano-MgO from the precursor. The acid leaching process resulted in the great development of pore structures, which increased the specific surface area and achieved a high degree of dispersion and exposure of Cu atoms in the Cu-N_2-C active sites. In a nutshell, the defect structures and the content of the coordination functional group in the direct structure of the carrier have a great influence. The pretreatment of the structure defect site of the carrier is advantageous to directly construct the UM-N_x-C active sites of SACs.

4.3.2 Indirect construction method

The construction of SACs with UM-N_x-C active sites by indirect construction methods is also widely studied. UM-N_x-C active sites can be formed through the modification of the coordination of metal atoms with N atoms. The SACs with UM-N_x-C active sites were obtained by secondary calcination or other treatment. It is found that the secondary high-temperature pyrolysis of the SACs affects the local electron density and valence state of the metal atoms. It also helps accelerate the dissociation of the carbon matrix to release nitrogen atoms, which are conducive to forming more pores. A small shift of the pyridine N peak of SACs in XPS spectra means that the secondary pyrolysis could promote the formation of the UM-N_x-C active sites between pyridine N and metal atom. Zhu et al.[161] found that the Fe-N_3-C active site was transferred to the Fe-N_5-C active site after high-temperature pyrolysis in a g-C_3N_4-based SAC. High-temperature pyrolysis provides energy for Fe atoms to migrate to the C-N vacancy to form a more stable Fe-N_5-C active site structure. The UM-N_x-C active site transformation also can be achieved through an N atom removal process.

Zhou et al[162]. prepared Fe-N_3-C active sites by secondary high-temperature pyrolysis of a zeolitic imidazolate framework (ZIF)-derived Fe-SAC. It is at-

tributed that pyridine N is more likely to bond to Fe atoms in the form of coordination bonds. Secondary pyrolysis greatly influences the electron density and pyridine N content of UM-N_x-C active sites. A modification of the ratio of M and N facilitates the formation of UM-N_x-C active sites[91,108,163].

4.3.3 Factors affecting the construction of UM-N_x-C active sites

4.3.3.1 Temperature

The temperature has a significant effect on the coordination number of N in the construction process of UM-N_x-C active sites, and the M-N_4-C active sites can be destroyed by secondary calcination at high temperatures to form the UM-N_x-C active sites. Han et al.[168] prepared a series of Ni-SACs by loading single-atom metals on N-doped carbon substrates by the solution-carbonization method, showing that the structure of carbon materials can be affected by changing calcination temperature. Furthermore, the M-N_x-C active sites attached to the carbon material are affected by the pyrolysis temperature. The change of Ni-N_x-C active site coordination number in the construction of Ni-SACs from MOF-derived carbons was investigated by changing the temperature from 800 to 1000 °C. With increasing the temperature, the coordination number of Ni-N_x-C active site centers decreased from 3.14 to 2.63, and the relative ratio of pyrrole N/pyridine N increased from 0.37 to 1.01. This may be due to the transformation of pyridine N to pyrrole N, which is the key factor for forming the M-N_x-C active site[169]. In addition, the machine learning algorithm can also recognize that the heating temperature during SAC synthesis has a significant effect on the M-N_x-C active site coordination number. The Fe-N_x-C active sites of SACs are closely related to the support construction and single-atom anchoring during the coordination process, which ultimately determines the catalytic performance of SACs. Through machine learning-guided optimization, the SAC dominated by the Fe-N_5-C active site was developed and showed excellent activity in the SACs/Fenton-like system[170]. In short, SACs containing the active site of UM-N_x-C active sites may be more easily obtained by pyrolysis of carbon materials with high N contents at high temperatures.

4.3.3.2 Carrier regulation

(1) Effect of defect degree

The distribution of metal particle size and the single metal site can be precisely adjusted by adjusting the molar ratio of Zn/M in the ZIF carbon carrier and the annealing temperature during post-treatment, which are beneficial to the formation of the active site of UM-N_x-C active sites on the SACs[171–172]. This effect may be because the evaporation of Zn atoms at high temperatures (> 900 °C) results in more metal vacancies and defects in the original carbon carrier. The increased surface area of the support facilitates the exposure of metal atoms, which are more readily contacted with nitrogen-containing functional groups to form the UM-N_x-C active site[173].

(2) Effect of N regulation

It was found that the more N-containing functional groups (mainly pyrrole N and pyridine N), the more favorable the formation of SACs containing UM-N_x-C active sites after pyrolysis at high temperatures. It is likely that the high temperature has destroyed the coordination structure between the N-containing functional group and the carbon carrier and changed the coordination number of N to form a new M-N_x-C active site. The synergy of UM-N_x-C and N-containing functional groups could also greatly reduce the migration distance of the oxidized species through the PMS activation. PMS tends to bind to the UM-N_x-C site, leading to rapid electron accumulation and depletion, thereby efficiently activating PMS to produce $^1O_2$. Meanwhile, contaminants adsorb onto the pyrrolic N site by a “donor-receptor complex” mechanism. The dual reaction sites within the SACs greatly reduce the migration distance of the active $^1O_2$[65,174–175].

Modifying the carrier also led to form more UM-N_x-C active sites on the SACs. Miao et al.[162] regulated the N coordination number in the Mn-N_x-C active sites by adding NH_4Cl to the carrier. It was found that a SAC containing the Mn-N_5-C active site could be formed after adding NH_4Cl to the g-C_3N_4 support,

which could activate PMS more effectively than a SAC containing the Mn-N_4-C active site.

Therefore, the regulation of the pyrrole N and pyridine N content would greatly improve the formation of UM-N_x-C active sites. Adding N sources to the carbon-containing carriers and pyrolysis at high temperatures can lead to more N-containing functional groups, resulting in the formation of more M-N_x-C active sites on the carbon-derived materials[48,163].

5 Conclusions and outlook

5.1 Conclusions

PS can be effectively activated by M-N_x-C active sites on SACs to produce non-radical species for deep mineralization or selective removal of organic contaminants in complex waters. However, the role and the construction method of different M-N_x-C active sites, especially UM-N_x-C active sites, for the non-radical activation of PS has not been systematically reviewed. In this review, the mechanism of PS activation by the M-N_x-C active site, the construction methods, and the effect of the carrier of the M-N_x-C active sites were analyzed systematically. Moreover, the factors affecting the UM-N_x-C active sites were also summarized. The main conclusions are described below.

(1) The mechanism of SACs activating PS mainly involves $^1O_2$, ETP and HVMO. The M-N_4-C active sites are important in the "Donor-receptor complex" mechanism. The M-N_4-C active sites could significantly trigger S—O bond breakage and O—O bond polarization of PS and form a non-radical PS intermediate through the adsorption of PS and contaminants on it. UM-N_x-C active sites would greatly affect the electron density of the metal atom and decrease the surface atomic oxygen barrier, which could significantly improve the activity of SACs on PS activation.

(2) MOFs, g-C_3N_4, COFs, and biomass carbons are good carriers for M-N_x-C active site construction. Owing to their defect-rich structures, g-C_3N_4 and biomass carbons could be used to attain a high concentration of M-N_x-C active sites. Because of their highly adjustable structure, MOFs and COFs can be used as carriers to prepare SACs with complex structures.

(3) The construction of SACs with M-N_4-C active sites is mainly achieved using ALD, co-precipitation and impregnation. The ALD method can precisely control the concentration of active sites in SACs, while co-precipitation and impregnation methods allow for the convenient construction of large quantities of SACs, but it isn't easy to control the structure of the sites accurately. The construction of UM-N_x-C active sites is primarily achieved through direct and indirect methods. The indirect method, namely calcination of M-N_4-C active sites, is more controllable to form the UM-N_x-C active sites.

(4) The defect degree and N-containing functional groups (pyrrole N, pyridine N, and graphite N) significantly impact the construction of UM-N_x-C active sites. Among them, high temperatures can increase the defect degree of the support, and more pyrrole N and pyridine N are beneficial for the formation of UM-N_x-C active sites.

5.2 Outlook

M-N_x-C active sites have been extensively utilized for the non-radical activation of PS in SACs to remove organic contaminants from wastewater. However, the following points should be considered in future research:

(1) Much research reported are focused on the activation mechanism of M-N_x-C active sites to PMS through non-radical pathways. PDS is a cheaper and more effective oxidant, but the research about M-N_x-C active site construction for PDS activation is still insufficient. The activation mechanism of M-N_x-C active sites to PDS is not clear. Therefore, it is necessary to recognize the importance of the interactions between PDS and the M-N_x-C active sites.

(2) At present, most of the carbon carriers proposed are made of organic compounds, which is expensive and the preparing processes are usually energy-intensive. Carbon materials derived from solid waste, such as biomass carbon and gasification slag, are cheap and readily available. These materials are

expected to become promising supports for SACs in the non-radical activation of PS, especially when combined with new methods for defect creation.

(3) Secondary calcination is an effective method for indirectly constructing UM-N_x-C active sites. However, the transformation process from M-N_4-C to UM-N_x-C active sites are still unclear, leading to a complex construction method. More studies are needed to be done about the transformation mechanisms to simplify the construction of UM-N_x-C active sites.

(4) Degradation of organic contaminants through non-radical pathways has a better anti-interference performance, which is suitable for high-salinity wastewater. Systematical works should be carried out with PS activation on M-N_x-C active sites in real high-salinity wastewater, such as concentrated wastewater from membrane treatment.

(5) In order to better control the active sites during the preparation process of SACs, it is necessary to develop in-situ or semi-in-situ characterization techniques, such as in-situ IR and in-situ Raman.

Acknowledgements

The authors would like to acknowledge the financial support from the autonomous research project of SKLCC (2024BWZ005), the Youth Innovation Promotion Association of the Chinese Academy of Sciences (2022174, Z.Z.Q.), the Science and Technology Major Project of Shanxi Province (202005D121002), Fundamental Research Program of Shanxi Province (202303021212376), the Special Research Assistant Program of the Chinese Academy of Sciences (2023, Q.F.), ICC CAS (SCJC-WRW-2022-19), and Fundamental Research Program of Shanxi Province (202103021224443).

Author information

***Corresponding authors:**

Fei QI, Associate researcher. E-mail: qifei@sxicc.ac.cn;

CHEN Jia-bin, Professor. E-mail: chenjiabin@tongji.edu.cn;

ZENG Ze-quan, Associate researcher. E-mail: zengzequan@sxicc.ac.cn;

HUANG Zhang-gen, Professor. E-mail: zghuang@sxicc.ac.cn

First author:

SI Wen-hao. E-mail: 13555855295@163.com

References

[1] Al-Tohamy R, Ali S S, Li F, et al. A critical review on the treatment of dye-containing wastewater: Ecotoxicological and health concerns of textile dyes and possible remediation approaches for environmental safety[J]. Ecotoxicology and Environment Safety, 2022, 231: 113160.

[2] Patel M, Kumar R, Kishor K, et al. Pharmaceuticals of emerging concern in aquatic systems: Chemistry, occurrence, effects, and removal methods[J]. Chemical Reviews, 2019, 119(6): 3510-3673.

[3] Sharma J, Sharma S, Soni V. Classification and impact of synthetic textile dyes on aquatic flora: A review[J]. Regional Studies in Marine Science, 2021, 45.

[4] Qi F, Chen J, Zeng Z, et al. Periodate activation with polyaniline-derived carbon for bisphenol a degradation: Insight into the roles of nitrogen dopants and non-radical species formation[J]. Chemical Engineering Journal, 2024, 499.

[5] Yang L, He L, Xue J, et al. Persulfate-based degradation of perfluorooctanoic acid (PFOA) and perfluorooctane sulfonate (PFOS) in aqueous solution: Review on influences, mechanisms and prospective[J]. Journal of Hazardous Materials, 2020, 393: 122405.

[6] Zheng X, Niu X, Zhang D, et al. Metal-based catalysts for persulfate and peroxymonosulfate activation in heterogeneous ways: A review[J]. Chemical Engineering Journal, 2022, 429.

[7] Ma C, Guo Y, Zhang D, et al. Metal-nitrogen-carbon catalysts for peroxymonosulfate activation to degrade aquatic organic contaminants: Rational design, size-effect description, applications and mechanisms[J]. Chemical Engineering Journal, 2023, 454.

[8] Giannakis S, Lin K Y A, Ghanbari F. A review of the recent advances on the treatment of industrial wastewaters by sulfate radical-based advanced oxidation processes (SR-AOPs)[J]. Chemical Engineering Journal, 2021, 406.

[9] Guan Y H, Ma J, Li X C, et al. Influence of ph on the formation of sulfate and hydroxyl radicals in the uv/peroxymonosulfate system[J]. Environmental Science & Technology, 2011, 45(21): 9308-9314.

[10] Zhai C, Chen Y, Huang X, et al. Recent progress on single-atom catalysts in advanced oxidation processes for water treatment[J]. Environmental Functional Materials, 2022, 1(3): 219-229.

[11] Zhu Z S, Wang P, Liu Y, et al. Microenvironment modulation of carbon-based single-atom catalysts for advanced oxidation processes[J]. Environmental Functional Materials, 2025.

[12] Wen Q, Qi F, Wang S, et al. Persulfate activation by Fe, N co-

doped carbon: Effect of N-containing groups on electron structure of Fe-N sites[J]. Environmental Functional Materials, 2024, 3(1): 34-45.

[13] Khan A, Liao Z, Liu Y, et al. Synergistic degradation of phenols using peroxymonosulfate activated by CuO-Co(3)O(4)@MnO(2) nanocatalyst[J]. Journal of Hazardous Materials, 2017, 329: 262-271.

[14] Han F, Ye X, Chen Q, et al. The oxidative degradation of diclofenac using the activation of peroxymonosulfate by $BiFeO_3$ microspheres —Kinetics, role of visible light and decay pathways[J]. Separation and Purification Technology, 2020, 232.

[15] Li Y, Qi J, Shen J, et al. Non-radical dominated degradation of bisphenol S by peroxymonosulfate activation under high salinity condition: Overlooked HOCl, formation of intermediates, and toxicity assessment[J]. Journal of Hazardous Materials, 2022, 435: 128968.

[16] Chen N, Fang G, Zhu C, et al. Surface-bound radical control rapid organic contaminant degradation through peroxymonosulfate activation by reduced Fe-bearing smectite clays[J]. Journal of Hazardous Materials, 2020, 389: 121819.

[17] Duan X, Ao Z, Zhou L, et al. Occurrence of radical and nonradical pathways from carbocatalysts for aqueous and nonaqueous catalytic oxidation[J]. Applied Catalysis B: Environmental, 2016, 188: 98-105.

[18] Zhao X, An Q-D, Xiao Z-Y, et al. Seaweed-derived multifunctional nitrogen/cobalt-codoped carbonaceous beads for relatively high-efficient peroxymonosulfate activation for organic pollutants degradation[J]. Chemical Engineering Journal, 2018, 353: 746-759.

[19] Zhou Y, Jiang J, Gao Y, et al. Activation of peroxymonosulfate by benzoquinone: A novel nonradical oxidation process[J]. Environmental Science and Technology, 2015, 49(21): 12941-12950.

[20] Duan X, Sun H, Shao Z, et al. Nonradical reactions in environmental remediation processes: Uncertainty and challenges[J]. Applied Catalysis B: Environmental, 2018, 224: 973-982.

[21] Du N, Liu Y, Li Q, et al. Peroxydisulfate activation by atomically-dispersed Fe-Nx on N-doped carbon: Mechanism of singlet oxygen evolution for nonradical degradation of aqueous contaminants[J]. Chemical Engineering Journal, 2021, 413.

[22] Huang Z, Cao K, Liu G, et al. Construction of a multiple reactive species-mediated Co_9S_8/NBC-PMS Fenton-like system for tetracycline degradation with broadened adaptability to water background[J]. Journal of Environmental Chemical Engineering, 2024, 12(6).

[23] Peng X, Wu J, Zhao Z, et al. Activation of peroxymonosulfate by single atom Co-N-C catalysts for high-efficient removal of chloroquine phosphate via non-radical pathways: Electron-transfer mechanism[J]. Chemical Engineering Journal, 2022, 429.

[24] Liu X, Pei Y, Cao M, et al. Highly dispersed copper single-atom catalysts activated peroxymonosulfate for oxytetracycline removal from water: Mechanism and degradation pathway[J]. Chemical Engineering Journal, 2022, 450.

[25] Kang J, Zhang H, Duan X, et al. Nickel in hierarchically structured nitrogen-doped graphene for robust and promoted degradation of antibiotics[J]. Journal of Cleaner Production, 2019, 218: 202-211.

[26] Zhou X, Zhao Q, Wang J, et al. Nonradical oxidation processes in PMS-based heterogeneous catalytic system: Generation, identification, oxidation characteristics, challenges response and application prospects[J]. Chemical Engineering Journal, 2021, 410.

[27] Gao Y, Zhu Y, Li T, et al. Unraveling the high-activity origin of single-atom iron catalysts for organic pollutant oxidation via peroxymonosulfate activation[J]. Environmental Science and Technology, 2021, 55(12): 8318-8328.

[28] Miao W, Liu Y, Wang D, et al. The role of Fe-N_x single-atom catalytic sites in peroxymonosulfate activation: Formation of surface-activated complex and non-radical pathways[J]. Chemical Engineering Journal, 2021, 423.

[29] Cheng C, Ren W, Zhang H, et al. Single-atom iron catalysts for peroxymonosulfate-based advanced oxidation processes: Coordination structure versus reactive species[J]. Chinese Journal of Catalysis, 2024, 59: 15-37.

[30] Li H, Shan C, Pan B. Fe(III)-doped g-C_3N_4 mediated peroxymonosulfate activation for selective degradation of phenolic compounds via high-valent iron-Oxo Species[J]. Environmental Science and Technology, 2018, 52(4): 2197-2205.

[31] Du X, Zhang Y, Si F, et al. Persulfate non-radical activation by nano-CuO for efficient removal of chlorinated organic compounds: Reduced graphene oxide-assisted and CuO (0 0 1) facet-dependent[J]. Chemical Engineering Journal, 2019, 356: 178-189.

[32] Ahn Y-Y, Bae H, Kim H-I, et al. Surface-loaded metal nanoparticles for peroxymonosulfate activation: Efficiency and mechanism reconnaissance[J]. Applied Catalysis B: Environmental, 2019, 241: 561-569.

[33] Zhao H, Liu Y, Wu D, et al. Multi-pathway on peroxymonosulfate activation by single cobalt atoms incorporated on CuO with enriched oxygen vacancies for high-efficient oxidation of tetracycline[J]. Environmental Pollution, 2023, 335: 122298.

[34] Chen L, Xing K, Shentu Q, et al. Well-dispersed iron and nitrogen co-doped hollow carbon microsphere anchoring by g-C_3N_4 for efficient peroxymonosulfate activation[J]. Chemosphere, 2021, 280: 130911.

[35] Guo X, Zhang Q, He H, et al. Wastewater flocculation substrate derived three-dimensional ordered macroporous Co single-atom catalyst for singlet oxygen-dominated peroxymonosulfate activation[J]. Applied Catalysis B: Environmental, 2023, 335.

[36] Xiao G, Xu T, Faheem M, et al. Evolution of singlet oxygen by activating peroxydisulfate and peroxymonosulfate: A review[J]. Int J Environ Res Public Health, 2021, 18(7).

[37] Yang T, Fan S, Li Y, et al. Fe-N/C single-atom catalysts with high density of Fe-N_x sites toward peroxymonosulfate activation for high-efficient oxidation of bisphenol A: Electron-transfer

mechanism[J]. Chemical Engineering Journal, 2021, 419.

[38] Li F, Lu Z, Li T, et al. Origin of the excellent activity and selectivity of a single-atom copper catalyst with unsaturated Cu-N_2 sites via peroxydisulfate activation: Cu(III) as a dominant oxidizing species[J]. Environmental Science and Technology, 2022, 56(12): 8765-8775.

[39] Wang Q, Liu C, Zhou D, et al. Degradation of bisphenol a using peroxymonosulfate activated by single-atomic cobalt catalysts: Different reactive species at acidic and alkaline pH[J]. Chemical Engineering Journal, 2022, 439.

[40] Yang M, Hou Z, Zhang X, et al. Unveiling the origins of selective oxidation in single-atom catalysis via Co-N_4-C intensified radical and nonradical pathways[J]. Environmental Science and Technology, 2022, 56(16): 11635-11645.

[41] Yin K, Shang Y, Chen D, et al. Redox potentials of pollutants determining the dominate oxidation pathways in manganese single-atom catalyst (Mn-SAC)/peroxymonosulfate system: Selective catalytic mechanisms for versatile pollutants[J]. Applied Catalysis B: Environmental, 2023, 338.

[42] Tang L, Liu Y, Wang J, et al. Enhanced activation process of persulfate by mesoporous carbon for degradation of aqueous organic pollutants: Electron transfer mechanism[J]. Applied Catalysis B: Environmental, 2018, 231: 1-10.

[43] Wang H, Guo W, Liu B, et al. Edge-nitrogenated biochar for efficient peroxydisulfate activation: An electron transfer mechanism[J]. Water Research, 2019, 160: 405-414.

[44] Ye S, Zeng G, Tan X, et al. Nitrogen-doped biochar fiber with graphitization from Boehmeria nivea for promoted peroxymonosulfate activation and non-radical degradation pathways with enhancing electron transfer[J]. Applied Catalysis B: Environmental, 2020, 269.

[45] Dong J, Xu W, Liu S, et al. Recent advances in applications of nonradical oxidation in water treatment: Mechanisms, catalysts and environmental effects[J]. Journal of Cleaner Production, 2021, 321.

[46] Yu Y, Tan P, Huang X, et al. Homogeneous activation of peroxymonosulfate using a low-dosage cross-bridged cyclam manganese(II) complex for organic pollutant degradation via a nonradical pathway[J]. Journal of Hazardous Materials, 2020, 394: 122560.

[47] Ye P, Wang M, Wei Y, et al. Mechanochemical formation of highly active manganese species from OMS-2 and peroxymonosulfate for degradation of dyes in aqueous solution[J]. Research on Chemical Intermediates, 2018, 45(3): 935-946.

[48] Peng L, Duan X, Shang Y, et al. Engineered carbon supported single iron atom sites and iron clusters from Fe-rich Enteromorpha for Fenton-like reactions via nonradical pathways[J]. Applied Catalysis B: Environmental, 2021, 287.

[49] Li Y, Yang T, Qiu S, et al. Uniform N-coordinated single-atomic iron sites dispersed in porous carbon framework to activate PMS for efficient BPA degradation via high-valent iron-oxo species[J]. Chemical Engineering Journal, 2020, 389.

[50] Wang S, Xia Y, Tan L, et al. Co and N co-doped hierarchical porous carbon as peroxymonosulfate activator for phenol degradation via nonradical pathway mechanism[J]. Colloids and Surfaces A: Physicochemical and Engineering Aspects, 2022, 655.

[51] Duan P, Pan J, Du W, et al. Activation of peroxymonosulfate via mediated electron transfer mechanism on single-atom Fe catalyst for effective organic pollutants removal[J]. Applied Catalysis B: Environmental, 2021, 299.

[52] Xin S, Ni L, Zhang P, et al. Electron delocalization realizes speedy fenton-like catalysis over a high-loading and low-valence zinc single-atom catalyst[J]. Adv Sci (Weinh), 2023, 10(34): e2304088.

[53] Pan J, Gao B, Duan P, et al. Improving peroxymonosulfate activation by copper ion-saturated adsorbent-based single atom catalysts for the degradation of organic contaminants: electron-transfer mechanism and the key role of Cu single atoms[J]. Journal of Materials Chemistry A, 2021, 9(19): 11604-11613.

[54] Liu X, Huang D, Lai C, et al. Single cobalt atom anchored on carbon nitride with cobalt nitrogen/oxygen active sites for efficient Fenton-like catalysis[J]. Journal of Colloid and Interface Science, 2023, 629(Pt B): 417-427.

[55] Xu X, Zhan F, Pan J, et al. Engineering single-atom Fe-Pyridine N(4) sites to boost peroxymonosulfate activation for antibiotic degradation in a wide pH range[J]. Chemosphere, 2022, 294: 133735.

[56] Zhu W, Ndayiragije S, Zuo X, et al. ZIF-8-derived single-atom Cu and N co-coordinated porous carbon as bifunctional material for SMX removal[J]. Journal of Environmental Chemical Engineering, 2022, 10(3).

[57] Yang C, Shang S S, Fan Y, et al. Incorporation of atomically dispersed cobalt in the 2D metal-organic framework of a lamellar membrane for highly efficient peroxymonosulfate activation[J]. Applied Catalysis B-Environment and Energy, 2023, 325.

[58] Meng H, Zhou J, Zhang Y, et al. Single-atom Co-N_3 sites induce peroxymonosulfate activation for acetaminophen degradation via nearly 100 % internal electron transfer process[J]. Applied Catalysis B: Environment and Energy, 2025, 366.

[59] Fang X, Feng Y, Li X, et al. Efficient Fenton-like catalysis enabled by single cobalt atoms anchored on expanded graphite: Remarkable intrinsic activity of Co-N_4 sites and the enhanced mass transfer facilitated by gradient mesopore structure[J]. Chemical Engineering Journal, 2024, 479.

[60] Gao Y, Wu T, Yang C, et al. Activity trends and mechanisms in peroxymonosulfate-assisted catalytic production of singlet oxygen over atomic metal-N-C catalysts[J]. Angewandte Chemie, International Edition in English, 2021, 60(41): 22513-22521.

[61] Xie M, Yao M, Zhang S, et al. Single-atom Co-N_5 catalytic sites on carbon nanotubes as peroxymonosulfate activator for sulfamerazine degradation via enhanced electron transfer pathway[J]. Separation and Purification Technology, 2023, 304.

[62] Li Z, Ji S, Liu Y, et al. Well-defined materials for heterogeneous catalysis: From nanoparticles to isolated single-atom sites[J]. Chemical Reviews, 2020, 120(2): 623-682.

[63] Mi X, Wang P, Xu S, et al. Almost 100% peroxymonosulfate conversion to singlet oxygen on single-atom CoN(2+2) sites[J]. Angewandte Chemie, International Edition in English, 2021, 60(9): 4588-4593.

[64] Wang B, Cheng C, Jin M, et al. A site distance effect induced by reactant molecule matchup in single-atom catalysts for fenton-like reactions[J]. Angewandte Chemie, International Edition in English, 2022, 61(33): e202207268.

[65] Li X, Huang X, Xi S, et al. Single cobalt atoms anchored on porous N-doped graphene with dual reaction sites for efficient fenton-like catalysis[J]. Journal of the American Chemical Society, 2018, 140(39): 12469-12475.

[66] Yang J, Zeng D, Zhang Q, et al. Single Mn atom anchored on N-doped porous carbon as highly efficient Fenton-like catalyst for the degradation of organic contaminants[J]. Applied Catalysis B: Environmental, 2020, 279.

[67] Wang J, Bi S, Zhang Y, et al. Single-atom coordination-dependent catalysis for peroxymonosulfate-mediated water purification[J]. Current Opinion in Chemical Engineering, 2023, 41.

[68] Liang X, Fu N, Yao S, et al. The progress and outlook of metal single-atom-site catalysis[J]. Journal of the American Chemical Society, 2022, 144(40): 18155-18174.

[69] Yang J, Li P, Duan X, et al. Insights into the role of dual reaction sites for single Ni atom Fenton-like catalyst towards degradation of various organic contaminants[J]. Journal of Hazardous Materials, 2022, 430: 128463.

[70] Wang Y, Zuo S, Zeng C, et al. Unraveling the single-atom Fe-N(4) catalytic site selectivity generates singlet oxygen via activation of persulfate: Polarizing electric fields changes the electron transfer pathway[J]. Chemosphere, 2023, 344: 140331.

[71] Jiang N, Xu H, Wang L, et al. Nonradical oxidation of pollutants with single-atom-Fe(III)-activated persulfate: Fe(V) being the possible intermediate oxidant[J]. Environmental Science and Technology, 2020, 54(21): 14057-14065.

[72] Wang Z, Bao J, He H, et al. Single-atom iron catalyst activating peroxydisulfate for efficient organic contaminant degradation relying on electron transfer[J]. Chemical Engineering Journal, 2023, 458.

[73] Zhou C, Liang Y, Xia W, et al. Single atom Mn anchored on N-doped porous carbon derived from spirulina for catalyzed peroxymonosulfate to degradation of emerging organic pollutants[J]. Journal of Hazardous Materials, 2023, 441: 129871.

[74] Kim K, Kim G, Jeong T, et al. Activating the Mn single atomic center for an efficient actual active site of the oxygen reduction reaction by spin-state regulation[J]. Journal of the American Chemical Society, 2024, 146(49): 34033-34042.

[75] Zhang J, Li F, Liu W, et al. Modulating spin of atomic manganese center for high-performance oxygen reduction reaction[J]. Angewandte Chemie International Edition, 2024, 63(51).

[76] Miao J, Song J, Lang J, et al. Single-atom MnN(5) catalytic sites enable efficient peroxymonosulfate activation by forming highly reactive Mn(IV)-oxo species[J]. Environmental Science and Technology, 2023, 57(10): 4266-4275.

[77] Guo Z Y, Li C X, Gao M, et al. Mn−O covalency governs the intrinsic activity of Co-Mn spinel oxides for boosted peroxymonosulfate activation[J]. Angewandte Chemie International Edition, 2020, 60(1): 274-280.

[78] Zhang T, Lowry G V, Capiro N L, et al. In situremediation of subsurface contamination: Opportunities and challenges for nanotechnology and advanced materials[J]. Environmental Science: Nano, 2019, 6(5): 1283-1302.

[79] Yang Q, Jia Y, Wei F, et al. Understanding the activity of Co-N(4-x) C(x) in atomic metal catalysts for oxygen reduction catalysis[J]. Angewandte Chemie, International Edition in English, 2020, 59(15): 6122-6127.

[80] Zhong W, Qiu Y, Shen H, et al. Electronic spin moment as a catalytic descriptor for Fe single-atom catalysts supported on C(2)N[J]. Journal of the American Chemical Society, 2021, 143(11): 4405-4413.

[81] Zhou S, Miao X, Zhao X, et al. Engineering electrocatalytic activity in nanosized perovskite cobaltite through surface spin-state transition[J]. Nature Communications, 2016, 7: 11510.

[82] Sun Y, Sun S, Yang H, et al. Spin-related electron transfer and orbital interactions in oxygen electrocatalysis[J]. Advanced Materials, 2020, 32(39): e2003297.

[83] Miao J, Zhu Y, Lang J, et al. Spin-state-dependent peroxymonosulfate activation of single-atom M–N moieties via a radical-free pathway[J]. ACS Catalysis, 2021, 11(15): 9569-9577.

[84] Zhang B, Li X, Akiyama K, et al. Elucidating the mechanistic origin of a spin state-dependent FeN(x)-C catalyst toward organic contaminant oxidation via peroxymonosulfate activation[J]. Environmental Science and Technology, 2022, 56(2): 1321-1330.

[85] Duan P, Li M, Xu X, et al. Understanding of interfacial molecular interactions and inner-sphere reaction mechanism in heterogeneous Fenton-like catalysis on Mn-N_4 site[J]. Applied Catalysis B: Environmental, 2024, 344.

[86] Jia Y, Chen Y, Xue Y, et al. Efficient activation of peroxymonosulfate by Mn single-atom: Critical role of Mn-N_4 coordination for generating singlet oxygen[J]. Separation and Purification Technology, 2024, 335.

[87] Cheng C, Ren W, Miao F, et al. Generation of Fe(IV) =O and its contribution to fenton-like reactions on a single-atom iron-N-C catalyst[J]. Angewandte Chemie, International Edition in English, 2023, 62(10): e202218510.

[88] Xu H, Cheng D, Cao D, et al. A universal principle for a rational design of single-atom electrocatalysts[J]. Nature Catalysis, 2018, 1(5): 339-348.

[89] Liang X, Wang D, Zhao Z, et al. Engineering the low-coordinated single cobalt atom to boost persulfate activation for enhanced organic pollutant oxidation[J]. Applied Catalysis B: Environmental, 2022, 303.

[90] Liang X, Wang D, Zhao Z, et al. Coordination number dependent catalytic activity of single-atom cobalt catalysts for fenton-like reaction[J]. Advanced Functional Materials, 2022, 32(38).

[91] Yin K, Wu R, Shang Y, et al. Microenvironment modulation of

cobalt single-atom catalysts for boosting both radical oxidation and electron-transfer process in Fenton-like system[J]. Applied Catalysis B: Environmental, 2023, 329.

[92] Huang K, Wei Z, Liu J, et al. Engineering the morphology and microenvironment of a graphene-supported Co-N-C single-atom electrocatalyst for enhanced hydrogen evolution[J]. Small, 2022, 18(19): e2201139.

[93] Ma W, Ren X, Li J, et al. Advances in atomically dispersed metal and nitrogen co-doped carbon catalysts for advanced oxidation technologies and water remediation: From microenvironment modulation to non-radical mechanisms[J]. Small, 2024, 20(22): e2308957.

[94] Zhao Y, Gao R, Wang H, et al. ZIF-8-derived hollow carbon polyhedra with highly accessible single Mn-N_6 sites as peroxymonosulfate activators for efficient sulfamethoxazole degradation[J]. Chemical Engineering Journal, 2023, 473.

[95] Qu W, Tang S, Tang Z, et al. Refining asymmetric low-coordinated Fe-N_3 motif to boost catalytic ozonation activity[J]. Advanced Functional Materials, 2024.

[96] Song X, Shi Y, Wu Z, et al. Unraveling the discriminative mechanisms for peroxy activation via atomically dispersed Fe-N_5 sites for tunable water decontamination[J]. Applied Catalysis B: Environmental, 2024, 340.

[97] Suyana P, Ganguly P, Nair B N, et al. Co_3O_4–C_3N_4 p–n nano-heterojunctions for the simultaneous degradation of a mixture of pollutants under solar irradiation[J]. Environmental Science: Nano, 2017, 4(1): 212-221.

[98] Yang C, Zhao Z Y, Wei H T, et al. DFT calculations for single-atom confinement effects of noble metals on monolayer g-C_3N_4 for photocatalytic applications[J]. RSC Adv, 2021, 11(7): 4276-4285.

[99] Liu Y, Zhou H, Jin C, et al. Bio-porphyrin supported single-atom iron catalyst boosting peroxymonosulfate activation for pollutants degradation: A Singlet Oxygen-dominated nonradical pathway[J]. Applied Catalysis B: Environmental, 2023, 338.

[100] Liu H, Fu Y, Chen S, et al. A layered g-C_3N_4 support Single-atom Fe-N_4 catalyst derived from hemin to Activate PMS for Selective degradation of electron-rich compounds via singlet oxygen species[J]. Chemical Engineering Journal, 2023, 474.

[101] Guo Z, Xie Y, Xiao J, et al. Single-Atom Mn-N_4 Site-catalyzed peroxone reaction for the efficient production of hydroxyl radicals in an acidic solution[J]. Journal of the American Chemical Society, 2019, 141(30): 12005-12010.

[102] Yan H, Lai C, Liu S, et al. Insight into the selective oxidation behavior of organic pollutants via Ni-N_4-C mediated electron transfer pathway[J]. Chemical Engineering Journal, 2023, 473.

[103] Liu S, Hu Y, Xu H, et al. Directional electron transfer in single-atom cobalt nanozyme for enhanced photo-Fenton-like reaction[J]. Applied Catalysis B: Environmental, 2023, 335.

[104] Chen Y, Zou H, Yan B, et al. Atomically dispersed Cu nanozyme with intensive ascorbate peroxidase mimic activity capable of alleviating ROS-mediated oxidation damage[J]. Adv Sci (Weinh), 2022, 9(5): e2103977.

[105] Wu S, Yang Z, Zhou Z, et al. Catalytic activity and reaction mechanisms of single-atom metals anchored on nitrogen-doped carbons for peroxymonosulfate activation[J]. Journal of Hazardous Materials, 2023, 459: 132133.

[106] Xi J, Jung H S, Xu Y, et al. Synthesis strategies, catalytic applications, and performance regulation of single-atom catalysts[J]. Advanced Functional Materials, 2021, 31(12).

[107] Alsharabasy A M, Pandit A, Farras P. Recent advances in the design and sensing applications of hemin/coordination polymer-based nanocomposites[J]. Advanced Materials, 2021, 33(2): e2003883.

[108] Wei Y S, Zhang M, Zou R, et al. Metal-organic framework-based catalysts with single metal sites[J]. Chemical Reviews, 2020, 120(21): 12089-12174.

[109] Jiao L, Jiang H-L. Metal-organic-framework-based single-atom catalysts for energy applications[J]. Chem, 2019, 5(4): 786-804.

[110] Sun T, Xu L, Wang D, et al. Metal organic frameworks derived single atom catalysts for electrocatalytic energy conversion[J]. Nano Research, 2019, 12(9): 2067-2080.

[111] Song Z, Zhang L, Doyle-Davis K, et al. Recent advances in mof-derived single atom catalysts for electrochemical applications[J]. Advanced Energy Materials, 2020, 10(38).

[112] Pan Y, Sun K, Liu S, et al. Core-shell ZIF-8@ZIF-67-derived CoP nanoparticle-embedded N-Doped carbon nanotube hollow polyhedron for efficient overall water splitting[J]. Journal of the American Chemical Society, 2018, 140(7): 2610-2618.

[113] Shang Y, Liu X, Li Y, et al. Boosting fenton-like reaction by reconstructed single Fe atom catalyst for oxidizing organics: Synergistic effect of conjugated π-π sp^2 structured carbon and isolated Fe-N_4 sites[J]. Chemical Engineering Journal, 2022, 446.

[114] Yang H, Zhang P, Yi X, et al. Constructing highly utilizable Fe-N_4 single-atom sites by one-step gradient pyrolysis for electroreduction of O_2 and CO_2[J]. Chemical Engineering Journal, 2022, 440.

[115] Wang Y, Wang J, Wei D, et al. A "MOF-Protective-Pyrolysis" Strategy for the Preparation of Fe-N-C Catalysts and the Role of Fe, N, and C in the Oxygen Reduction Reaction in Acidic Medium[J]. ACS Applied Materials & Interfaces, 2019, 11(39): 35755-35763.

[116] Geng K, He T, Liu R, et al. Covalent organic frameworks: Design, synthesis, and functions[J]. Chemical Reviews, 2020, 120(16): 8814-8933.

[117] Chen Y-J, Zhuo H-Y, Pan Y, et al. Triazine COF-supported single-atom catalyst (Pd1/trzn-COF) for CO oxidation[J]. Science China Materials, 2021, 64(8): 1939-1951.

[118] Wu Y, Wang R, Kim Y. Single-atom catalysts on covalent organic frameworks for energy applications[J]. ACS Applied Materials & Interfaces, 2024, 16: 66874-66899.

[119] Li C, Liu L, Kang J, et al. Pristine MOF and COF materials for advanced batteries[J]. Energy Storage Materials, 2020, 31: 115-134.

[120] Yan Y, He T, Zhao B, et al. Metal/covalent–organic frameworks-based electrocatalysts for water splitting[J]. Journal of Materials Chemistry A, 2018, 6(33): 15905-15926.

[121] Peng Q, Wen G, Yuan C, et al. Regulating the local electron density and adsorption energy of COF-based single copper sites for highly efficient Fenton-like photo-oxidation[J]. Journal of Materials Chemistry A, 2024.

[122] Liu M, Xu Q, Miao Q, et al. Atomic Co–N_4 and Co nanoparticles confined in COF@ZIF-67 derived core–shell carbon frameworks: bifunctional non-precious metal catalysts toward the ORR and HER[J]. Journal of Materials Chemistry A, 2022, 10(1): 228-233.

[123] Ding D, Yang S, Qian X, et al. Nitrogen-doping positively, whilst sulfur-doping negatively affect the catalytic activity of biochar for the degradation of organic contaminant[J]. Applied Catalysis B: Environmental, 2020, 263.

[124] Qian M, Lu M, Yan M, et al. Single-atom Co-N_3 sites supported on waste paper-derived active carbon for synergistic adsorption and catalytic degradation of antibiotics[J]. Journal of Environmental Chemical Engineering, 2023, 11(1).

[125] Zhou X, Ke M K, Huang G X, et al. Identification of Fenton-like active Cu sites by heteroatom modulation of electronic density[J]. Proc Natl Acad Sci U S A, 2022, 119(8).

[126] Yu J, Li J, Xu C-Y, et al. Modulating the d-band centers by coordination environment regulation of single-atom Ni on porous carbon fibers for overall water splitting[J]. Nano Energy, 2022, 98.

[127] Li T, Lu T, Li X, et al. Atomically dispersed Mo sites anchored on multichannel carbon nanofibers toward superior electrocatalytic hydrogen evolution[J]. ACS Nano, 2021, 15(12): 20032-20041.

[128] Peng X, Wu J, Zhao Z, et al. Activation of peroxymonosulfate by single-atom Fe-g-C_3N_4 catalysts for high efficiency degradation of tetracycline via nonradical pathways: Role of high-valent iron-oxo species and Fe–N_x sites[J]. Chemical Engineering Journal, 2022, 427.

[129] Wang X, Yang C, Wang X, et al. Green synthesis of a highly efficient and stable single-atom iron catalyst anchored on nitrogen-doped carbon nanorods for the oxygen reduction reaction[J]. ACS Sustainable Chemistry & Engineering, 2020, 9(1): 137-146.

[130] Chen Z, Zheng H, Zhang J, et al. Covalent organic frameworks derived single-atom cobalt catalysts for boosting oxygen reduction reaction in rechargeable Zn-Air batteries[J]. Journal of Colloid and Interface Science, 2024, 670: 103-113.

[131] Yu L Q, Xia W J, Ma W J, et al. Universal method to fabricate transition metal single-atom-anchored carbon with excellent oxygen reduction reaction activity[J]. ACS Applied Materials & Interfaces, 2021, 13(11): 13534-13540.

[132] Yang M, Wu R, Cao S, et al. Versatile pathways for oxidizing organics via peroxymonosulfate activation by different single atom catalysts confining with Fe–N_4 or Cu–N_4 sites[J]. Chemical Engineering Journal, 2023, 451.

[133] Li X, Rong H, Zhang J, et al. Modulating the local coordination environment of single-atom catalysts for enhanced catalytic performance[J]. Nano Research, 2020, 13(7): 1842-1855.

[134] Song Y, Guo R, Feng B, et al. Coordination number engineering of Zn single-atom sites for enhanced transfer hydrogenation performance[J]. Chemical Engineering Journal, 2023, 465.

[135] Li D, Zhang S, Li S, et al. Mechanism of the application of single-atom catalyst-activated PMS/PDS to the degradation of organic pollutants in water environment: A review[J]. Journal of Cleaner Production, 2023, 397.

[136] Fonseca J, Lu J. Single-atom catalysts designed and prepared by the atomic layer deposition technique[J]. ACS Catalysis, 2021, 11(12): 7018-7059.

[137] Lu J, Elam J W, Stair P C. Atomic layer deposition—sequential self-limiting surface reactions for advanced catalyst "bottom-up" synthesis[J]. Surface Science Reports, 2016, 71(2): 410-472.

[138] Zhang L, Banis M N, Sun X L. Single-atom catalysts by the atomic layer deposition technique[J]. National Science Review, 2018, 5(5): 628-+.

[139] George S M. Atomic layer deposition: An overview[J]. Chemical Reviews, 2010, 110(1): 111-131.

[140] Li J, Banis M N, Ren Z, et al. Unveiling the nature of Pt single-atom catalyst during electrocatalytic hydrogen evolution and oxygen reduction reactions[J]. Small, 2021, 17(11): e2007245.

[141] Stambula S, Gauquelin N, Bugnet M, et al. Chemical structure of nitrogen-doped graphene with single platinum atoms and atomic clusters as a platform for the PEMFC electrode[J]. The Journal of Physical Chemistry C, 2014, 118(8): 3890-3900.

[142] Wang X, Jin B, Jin Y, et al. Supported single Fe atoms prepared via atomic layer deposition for catalytic reactions[J]. ACS Applied Nano Materials, 2020, 3(3): 2867-2874.

[143] Zhang J, Yu J, Jaroniec M, et al. Noble metal-free reduced graphene oxide-$Zn_xCd(1)$-xS nanocomposite with enhanced solar photocatalytic H(2)-production performance[J]. Nano Letters, 2012, 12(9): 4584-4589.

[144] Lyu F, Zhang Y, Zare R N, et al. One-pot synthesis of protein-embedded metal-organic frameworks with enhanced biological activities[J]. Nano Letters, 2014, 14(10): 5761-5765.

[145] Xiong H, Datye A K, Wang Y. Thermally stable single-atom heterogeneous catalysts[J]. Advanced Materials, 2021, 33(50): e2004319.

[146] Zeng L, Chen J-W, Zhong L, et al. Synergistic effect of Ru-N_4 sites and Cu-N_3 sites in carbon nitride for highly selective photocatalytic reduction of CO_2 to methane[J]. Applied Catalysis B: Environmental, 2022, 307.

[147] Shi Y J, Guo X L, Wang Y Y, et al. New insight into the design of highly dispersed Pt supported CeO_2-TiO_2 catalysts with superior activity for VOCs low-temperature removal[J]. Green Energy & Environment, 2023, 8(6): 1654-1663.

[148] Yi M, Li N, Lu B, et al. Single-atom Pt decorated in heteroatom (N, B, and F)-doped ReS_2 Grown on Mo_2CT_x for efficient pH-universal hydrogen evolution reaction and flexible Zn–air batteries[J]. Energy Storage Materials, 2021, 42: 418-429.

[149] Hu S, Qiao P, Liu Z, et al. Porous C_3N_4 nanosheet supported Au single atoms as an efficient catalyst for enhanced photoreduction of CO_2 to CO[J]. Journal of Catalysis, 2024, 432.

[150] Wang J, Huang Y-C, Wang Y, et al. Atomically dispersed metal–nitrogen–carbon catalysts with d-orbital electronic configuration-dependent selectivity for electrochemical CO_2-to-CO reduction[J]. ACS Catalysis, 2023, 13(4): 2374-2385.

[151] Xia P, Wang C, He Q, et al. MOF-derived single-atom catalysts: The next frontier in advanced oxidation for water treatment[J]. Chemical Engineering Journal, 2023, 452.

[152] Wang Z, Almatrafi E, Wang H, et al. Cobalt single atoms anchored on oxygen-doped tubular carbon nitride for efficient peroxymonosulfate activation: simultaneous coordination structure and morphology modulation[J]. Angewandte Chemie, International Edition in English, 2022, 61(29): e202202338.

[153] Gao Y, Liu B, Wang D. Microenvironment engineering of single/dual-atom catalysts for electrocatalytic application[J]. Advanced Materials, 2023, 35(31): e2209654.

[154] Zhang L, Meng Q, Zheng R, et al. Microenvironment regulation of M-N-C single-atom catalysts towards oxygen reduction reaction[J]. Nano Research, 2023, 16(4): 4468-4487.

[155] Yang L, Yang H, Yin S, et al. Fe single-atom catalyst for efficient and rapid Fenton-like degradation of organics and disinfection against bacteria[J]. Small, 2022, 18(9): e2104941.

[156] Zhang X, Li C, Wang X, et al. Defect engineering modulated iron single atoms with assist of layered clay for enhanced advanced oxidation processes[J]. Small, 2022, 18(52): e2204793.

[157] Wang C, Wang X, Wang H, et al. Low-coordinated Co-N(3) sites induce peroxymonosulfate activation for norfloxacin degradation via high-valent cobalt-oxo species and electron transfer[J]. Journal of Hazardous Materials, 2023, 455: 131622.

[158] Qin Y, Ou Z, Xu C, et al. Highly accessible single Mn-N_3 sites-enriched porous graphene structure via a confined thermal-erosion strategy for catalysis of oxygen reduction[J]. Chemical Engineering Journal, 2022, 440.

[159] Xu F, Lai C, Zhang M, et al. High-loaded single-atom Cu-N_3 sites catalyze hydrogen peroxide decomposition to selectively induce singlet oxygen production for wastewater purification[J]. Applied Catalysis B: Environmental, 2023, 339.

[160] Tian S, Yin Y, Liu M, et al. Atomically dispersed Cu-N_3 on hollow spherical carbon nitride for acetaminophen degradation: Generation of $^1O_2$ from H_2O_2[J]. Separation and Purification Technology, 2023, 318.

[161] Zhu C, Nie Y, Cun F, et al. Two-step pyrolysis to anchor ultrahigh-density single-atom FeN_5 sites on carbon nitride for efficient Fenton-like catalysis near 0 °C[J]. Applied Catalysis B: Environmental, 2022, 319.

[162] Zhou Q, Lv N, Wang J, et al. The enhanced peroxymonosulfate activation ability and mechanism on low-coordinated Fe-N_3 single sites for organic pollutant degradation in wastewater[J]. Applied Surface Science, 2023, 640.

[163] Fei H, Dong J, Chen D, et al. Single atom electrocatalysts supported on graphene or graphene-like carbons[J]. Chemical Society Reviews, 2019, 48(20): 5207-5241.

[164] Yin Y, Li X, Li W N, et al. Atomically dispersed Co-N_4 to activate peroxymonosulfate for efficient atrazine degradation: Synergistic radical and non-radical ways[J]. Applied Surface Science, 2024, 661.

[165] Niu L, Tang Z, Lei Q, et al. Atomically dispersed Fe-N_4 sites in activation of peroxymonosulfate for wastewater purification: Mechanism of non-radical pathways and their quantification[J]. Chemical Engineering Journal, 2024, 499.

[166] Zeng Q, Wen Y, Duan X, et al. Single-atom Ni-N_4 sites coordinate dual nonradical oxidation pathways via peroxymonosulfate activation: Computational insights and in situ spectroscopic analyses[J]. Applied Catalysis B: Environmental, 2024, 346.

[167] Wang J, Ge X, Yin W, et al. Precise modulation of the coordination environment of single Cu site catalysts to regulate the peroxymonosulfate activation pathway for water remediation[J]. Inorganic Chemistry, 2024, 63(20): 9307-9314.

[168] Chen Y, Zhang R, Wang H T, et al. Temperature-dependent structures of single-atom catalysts[J]. Chem Asian J, 2023, 18(20): e202300679.

[169] Lim J W, Choo D H, Cho J H, et al. A MOF-derived pyrrolic N-stabilized Ni single atom catalyst for selective electrochemical reduction of CO_2 to CO at high current density[J]. Journal of Materials Chemistry A, 2024, 12(18): 11090-11100.

[170] Fu H, Li K, Zhang C, et al. Machine-learning-assisted optimization of a single-atom coordination environment for accelerated fenton catalysis[J]. ACS Nano, 2023, 17(14): 13851-13860.

[171] Wang X, Chen Z, Zhao X, et al. Regulation of coordination number over single Co sites: triggering the efficient electroreduction of CO(2)[J]. Angewandte Chemie, International Edition in English, 2018, 57(7): 1944-1948.

[172] Han X, Ling X, Wang Y, et al. Generation of nanoparticle, atomic-cluster, and single-atom cobalt catalysts from zeolitic imidazole frameworks by spatial isolation and their use in zinc-air batteries[J]. Angewandte Chemie, International Edition in English, 2019, 58(16): 5359-5364.

[173] Yin P, Yao T, Wu Y, et al. Single cobalt atoms with precise N-coordination as superior oxygen reduction reaction catalysts[J]. Angewandte Chemie, International Edition in English, 2016, 55(36): 10800-10805.

[174] Gawande M B, Fornasiero P, Zbořil R. Carbon-based single-atom catalysts for advanced applications[J]. ACS Catalysis, 2020, 10(3): 2231-2259.

[175] Peng Y, Lu B, Chen S. Carbon-supported single atom catalysts for electrochemical energy conversion and storage[J]. Advanced Materials, 2018, 30(48): e1801995.

单原子催化剂中 M-N_x-C 活性位点活化过硫酸盐产生非自由基途径的作用与构建方法

司文豪[1,2]，司锦轩[3]，王康军[2]，齐　菲[1,*]，陈家斌[4,*]，曾泽泉[1,*]，黄张根[1,5,*]

（1. 中国科学院山西煤炭化学研究所 煤炭高效低碳利用全国重点实验室，山西 太原 030001；
2. 沈阳化工大学 化学工程学院，辽宁 沈阳 110142；
3. 太原科技大学 化学工程技术学院，山西 太原 030024；
4. 同济大学 环境科学与工程学院，上海 200092；
5. 中国科学院大学，北京 100049）

摘　要： 由于单原子催化剂（SACs）高选择性和高活性的优势，大量的单原子催化剂（SACs）被合成并用于非自由基路径活化过硫酸盐（PS）。其中金属-氮-碳（M-N_x-C）结构被认为是 SACs 中的关键活性位点。尽管 SACs 制备方法已有深入的综述报道，但关于 M-N_x-C 特别是非常规金属-氮-碳（UM-N_x-C，$x\neq4$）结构在非自由基路径活化 PS 过程中的作用尚缺乏系统性的总结。本文综述了 M-N_x-C 活性位点在非自由基路径活化 PS 中的作用，介绍了 SACs 中 M-N_x-C 和 UM-N_x-C 活性位点的构建方法。探讨了催化剂载体如氮化碳（g-C_3N_4）、金属有机框架（MOFs）、共价有机框架（COFs）和其它炭材料对制备 SACs 的影响。详细总结了 UM-N_x-C 活性位点构建的直接和间接方法。最后讨论了在 SACs 上构建 M-N_x-C 活性位点的影响因素。本综述为设计具有 UM-N_x-C 活性位点的 SACs 提供了重要的参考，这些催化剂在活化 PS 通过非自由基途径降解复杂废水中的有机污染物方面具有良好的应用前景。

关键词： 单原子催化剂；过硫酸盐；非自由基路径；非常规金属-氮-碳活性位点；有机污染物

中图分类号： O64332　　**文献标识码：** A

基金项目： 煤炭高效低碳利用全国重点实验室自主研究课题资助项目 (2024BWZ005); 中国科学院青年创新促进会 (2022174,Z.Z.Q.); 山西省科技重大专项 (202005D121002); 山西省基础研究计划资助项目 (202303021212376); 中国科学院特别研究助理资助项目 (2023,Q.F.); 中国科学院山西煤炭化学研究所创新基金项基础研究项目 (SCJC-WRW-2022-19); 山西省基础研究计划资助项目 (22103021224443).

通讯作者： 齐　菲，助理研究员. E-mail: qifei@sxicc.ac.cn；
陈家斌，教授. E-mail: chenjiabin@tongji.edu.cn；
曾泽泉，副研究员. E-mail: zengzequan@sxicc.ac.cn；
黄张根，研究员. E-mail: zghuang@sxicc.ac.cn

第一作者： 司文豪. E-mail: 13555855295@163.com

本文的电子版全文由 Elsevier 出版社在 ScienceDirect 上出版（https://www.sciencedirect.com/journal/new-carbon-materials/）